



Published in final edited form as:

J Med Chem. 2009 August 27; 52(16): 5228–5240. doi:10.1021/jm900611t.

Structure-Based Design, Synthesis, and Biological Evaluation of a Series of Novel and Reversible Inhibitors for the Severe Acute Respiratory Syndrome-Coronavirus Papain-Like Protease

Arun K. Ghosh^{†,*}, Jun Takayama[†], Yoann Aubin[†], Kiira Ratia[‡], Rima Chaudhuri[‡], Yahira Baez[‡], Katrina Sleeman[‡], Melissa Coughlin^{‡,‡}, Daniel B. Nichols[‡], Debbie C. Mulhearn[‡], Bellur S. Prabhakar^{‡,‡}, Susan C. Baker[‡], Michael E. Johnson[‡], and Andrew D. Mesecar[‡]

[†]Departments of Chemistry and Medicinal Chemistry, Purdue University, West Lafayette, IN 47907

[‡]Center for Pharmaceutical Biotechnology and Department of Medicinal Chemistry and Pharmacognosy, University of Illinois at Chicago, 900 S. Ashland, IL

[‡]Department of Microbiology and Immunology, Loyola University of Chicago, Stritch School of Medicine, Maywood, IL 60153

^{‡,‡}Department of Microbiology and Immunology, University of Illinois, Chicago, IL 60607

Abstract

We describe here the design, synthesis, molecular modeling, and biological evaluation of a series of small molecule, nonpeptide inhibitors of SARS-CoV PL_{pro}. Our initial lead compound was identified via high-throughput screening of a diverse chemical library. We subsequently carried out structure-activity relationship studies, and optimized the lead structure to potent inhibitors that have shown antiviral activity against SARS-CoV infected Vero E6 cells. Based upon the X-ray crystal structure of one of the potent inhibitors **24**-bound to SARS-CoV PL_{pro}, a drug-design template was created. Our structure-based modification led to the design of a more potent inhibitor, **2** (enzyme IC₅₀ = 0.46 μM; antiviral EC₅₀ = 12.5 μM). Interestingly, its methylamine derivative **49** displayed good enzyme inhibitory potency (IC₅₀ = 1.3 μM) and most potent SARS antiviral activity (EC₅₀ = 2.5 μM) in the series. We have carried out computational docking studies and generated a predictive 3D-QSAR model for SARS-CoV PL_{pro} inhibitors.

Introduction

Severe Acute Respiratory Syndrome (SARS), a contagious and fatal respiratory illness, was first reported in Guangdong province, China, in November 2002.¹ It rapidly spread to other Asian countries, North America, and Europe, creating panic to both the public and the World Health Organization (WHO). The emergence of SARS affected more than 8000 individuals and caused 774 deaths within a few months.⁶ Quite remarkably, the spread of SARS-CoV was effectively halted within months after the initial outbreaks through public health measures. Through a concerted effort monitored by the WHO, scientists determined that SARS is caused by a novel coronavirus, SARS-CoV.^{2,3,3b} The more recent isolation of strains from zoonotic origins thought to be the reservoir for SARS-CoV, emphasizes the

*The corresponding author: Departments of Chemistry and Medicinal Chemistry, Purdue University, 560 Oval Drive, West Lafayette, IN 47907, Phone: (765)-494-5323; Fax: (765)-496-1612, akghosh@purdue.edu.

Supporting Information Available. HRMS and HPLC data of inhibitors and a stereoview of the X-ray structure of inhibitor **24**-bound SARS-CoV PL_{pro}. This material is available free of charge via the Internet at <http://pubs.acs.org>.

possibility of a reemergence.^{4,5} It is quite alarming just how rapidly a contagious illness can spread in the more mobile and highly interconnected world of the 21st century. While there are no new reports of SARS cases, there is no guarantee that this outbreak will not strike again. Therefore, development of antivirals effective against SARS-CoV is important for future outbreaks.

The identification of biochemical events critical to the coronaviral lifecycle has provided a number of significant targets for halting viral replication. One of the early and essential processes is the cleavage of a multidomain, viral polyprotein into 16 individual components termed non-structural proteins, or nsps. These proteins assemble into complexes to execute viral RNA synthesis.⁷ Two cysteine proteases, a papain-like protease (PLpro) and a 3C-like protease (3CLpro), reside within the polyprotein. They catalyze their own release and that of the other nsps from the polyprotein and initiate virus-mediated RNA replication. Since 2003, numerous biochemical, structural and inhibitor development studies have been directed at the 3CLpro enzyme⁸, which cleaves eleven sites within the polyprotein. Recently, we reported potent inhibitors of 3CLpro that have shown antiviral activity against SARS-CoV.⁹

Recent structural and functional studies directed at PLpro have suggested potential roles for this protease beyond viral peptide cleavage, including deubiquitination, deISGylation, and involvement in virus evasion of the innate immune response.^{10,11} Furthermore, studies have shown that the homologous enzyme, PLP2, from the human coronavirus 229E, is essential for 229E viral replication.¹² Therefore, PLpro has emerged as a significant drug development target. Our screening of a structurally diverse library of 50,080 compounds led to the discovery of a noncovalent lead inhibitor **1** (7724772, Figure 1), with an IC₅₀ value of 20 μM as a racemic mixture.¹³ Subsequent SAR studies and lead optimization provided potent inhibitor **24** (IC₅₀ = 600 nM) which also inhibits SARS-CoV viral replication in Vero cells with an EC₅₀ value of 15 μM.¹³ In these studies, we also reported the X-ray crystal structure of SARS-CoV PLpro bound to inhibitor **24**, which revealed important molecular insight into the ligand-binding site interactions. We now describe the full details of our significantly extended studies that include the design, synthesis, molecular modeling, and biological evaluation of a series of inhibitors of SARS-CoV PLpro.

Chemistry

As shown in Scheme 1, coupling of (*R*)-(+)-1-(2-naphthyl)ethylamine or (*R*)-(+)-1-(1-naphthyl)ethylamine with benzoic acid derivatives utilizing *N*-(3-dimethylaminopropyl)-*N'*-ethylcarbodiimide hydrochloride (EDCI), 1-hydroxybenzotriazole hydrate (HOBt) in the presence of diisopropylethylamine in CH₂Cl₂ at 23 °C gave the corresponding inhibitor in excellent yield. Inhibitors **8** and **9** were synthesized by general method with *N*-Boc protected benzoic acid derivative followed by deprotection of the Boc group as shown in Scheme 2. Protection of *p*-aminobenzoic acid **6** with di-*t*-butyl dicarbonate in the presence of triethylamine in a mixture (2:1) of dioxane and water at 23 °C for 16 h gave the corresponding *t*-Bu carbamate **7**.¹⁴ A coupling reaction utilizing EDCI and HOBt provided inhibitor **8**. Removal of the Boc group with trifluoroacetic acid in CH₂Cl₂ at 23 °C for 2 h afforded inhibitor **9**.

Inhibitors **14** and **17** were racemic compounds (Scheme 3). A Friedel-Crafts reaction of naphthalene **10** with propionyl chloride **11** in the presence of aluminum chloride in 1,2-dichloroethane at 35 °C for 4 h gave ethyl naphthyl ketone **12**.¹⁵ Reductive amination¹⁶ with ammonium acetate and sodium cyanoborohydride in methanol at 23 °C for 24 h generated amine **13**. Coupling of this amine with *o*-toluic acid provided inhibitor **14**. Reductive amination of naphthyl phenyl ketone **15** by using similar conditions as the amine **13** gave amine **16**. Coupling of **16** with *o*-toluic acid furnished inhibitor **17**.

Inhibitor **21** with *N*-methyl amide was prepared as shown in Scheme 4. Protection of (*R*)-(+)-1-(1-naphthyl)ethylamine **18** with methyl chloroformate in the presence of potassium carbonate in a mixture (1:1) of dioxane and water at 0 °C for 1 h afforded carbamate **19**. Reduction of **19** with lithium aluminum hydride in THF at reflux for 1 h gave methylamine **20**. A coupling reaction utilizing general methods provided inhibitor **21**. Inhibitor **23** was prepared by coupling of optically active amine **18** with acid **7** as shown.

Inhibitor **24** and **25** containing 2-methyl-5-amino derivatives were synthesized as outlined in Scheme 5. Reduction of the nitro group in **5i** by catalytic hydrogenation in the presence of 5% Pd-C in a mixture (1:1) of ethyl acetate and methanol at 23 °C for 15 h provided inhibitor **24**. Acetylation of **24** with acetic anhydride and triethylamine in CH₂Cl₂ at 23 °C for 18 h generated inhibitor **25**. The synthesis of inhibitor **29** with a gem dimethyl group in the α -naphthyl side chain was carried out by dimethylation of 1-cyanonaphthalene **26** with methyl lithium in the presence of cerium(III) chloride in tetrahydrofuran at 23 °C for 2 h to provide amine **27**.¹⁷ A coupling reaction using the general method described above provided **28**, and hydrogenation in the presence of 5% Pd-C in a mixture (1:1) ethyl acetate and methanol at 23 °C for 15 h provided inhibitor **29**.

The synthesis of **32** with 2-methyl-5-iodide and **33** with 2-methyl-5-cyanide substituents on the benzamide moiety is outlined in Scheme 6. Iodination of *o*-toluic acid **30** with sodium perchlorate and potassium iodide in concentrated sulfuric acid at 25–30 °C for 2 h afforded iodide **31**.¹⁸ The coupling reaction following the general method provided inhibitor **32** and cyanation with copper cyanide and sodium cyanide in DMF at 130 °C for 16 h furnished inhibitor **33**. Inhibitor **40** was synthesized by esterification of **34** in the presence of thionyl chloride in methanol at reflux for 4 h to provide ester **35**. Bromination of **35** with *N*-bromosuccinimide and benzoyl peroxide in carbon tetrachloride at reflux for 24 h generated bromide **36**.¹⁹ Reaction of **36** with sodium hydride and sodium methoxide in methanol at 50 °C for 16 h provided **37**.²⁰ Hydrolysis of **37** with lithium hydroxide monohydrate in a mixture (5:1) of tetrahydrofuran and water at 23 °C for 16 h afforded acid **38**. Coupling reaction with general method gave **39** and hydrogenation in the presence of 5% Pd-C in ethyl acetate at 23 °C for 10 h provided inhibitor **40**.

Inhibitors **47**, **49** and **2** have been synthesized as shown in Scheme 7. Reduction of nitro group in **35** by catalytic hydrogenation in the presence of 5% Pd-C in ethyl acetate at 23 °C for 15 h provided amine **41**. Reaction of **41** with sodium nitrite, copper cyanide and sodium cyanide in acidic condition at 23 °C for 3 h afforded corresponding benzonitrile **42**.²¹ Reduction and subsequent *N*-Boc protection with di-*t*-butyl dicarbonate and sodium borohydride in the presence of nickel (II) chloride hexahydrate in methanol at 23 °C for 2 h provided *N*-Boc-benzylamine **43**.²² *N*-Methylation with methyl iodide and potassium bis(trimethylsilyl)amide in tetrahydrofuran at 23 °C for 16 h afforded methylamine **44**. Hydrolysis of **43** with lithium hydroxide monohydrate in a mixture (9:1) of tetrahydrofuran and water at 23 °C for 16 h generated acid **45**. Coupling reaction of **45** with amine **18** using conditions described above provided inhibitor **47**. Removal of Boc-group with trifluoroacetic acid in dichloromethane at 23 °C for 2 h gave inhibitor **2**. Inhibitor **49** was prepared from benzylamine **44**. Ester hydrolysis, coupling of the resulting acid with amine **18** and subsequent removal of Boc-group as described for **2**, afforded inhibitor **49**.

Results and discussion

As described previously, screening of a library of 50,080 diverse compounds identified **1** as an inhibitor of PLpro activity.¹³ Since **1** is a racemic mix, we synthesized the corresponding chiral compounds to evaluate the stereospecific recognition of these compounds by PLpro. Compound, with the *R*-configuration, was found to be twice as potent as the racemic

compound **1** (*R*-configuration compound, $IC_{50} = 8.7 \mu\text{M}$; compound **1**, $IC_{50} = 20.1 \mu\text{M}$). We therefore selected *R*-configuration compound for further optimization as lead compound.

As shown in Table 1, we modified the substituent on the benzamide ring with methyl and methoxy groups. Compounds **5a–5e** turned out to be less potent than lead compound. Thus, a methyl group at the *ortho* position in lead compound displayed the most potent activity ($IC_{50} = 8.7 \mu\text{M}$). A methoxy group at the *ortho* position resulted in a 10-fold reduction in potency compared to lead compound. A methoxy group in the *meta* position (compound **5f**, $IC_{50} = 13.5 \mu\text{M}$) is the most potent analog among the methoxy substituted derivatives.

We next attempted further modification of the substituent on the benzamide as well as on the naphthyl rings, and the results are summarized in Table 2. As shown, a 2,6-dimethyl derivative, **5f**, led to an increase in the IC_{50} value compared to lead compound (compound **5f**, $IC_{50} = 12.1 \mu\text{M}$). Bulky substituents at the *ortho* and *para* positions of the benzamide ring and α -naphthyl position also resulted in increased IC_{50} values.

In an attempt to further improve the potency of PLpro inhibitors, we then examined 1-naphthalene derivatives and also explored polar functionalities on the benzamide ring based upon modeling studies. The results are shown in Table 3. Compound **5h**, with an *R*-1-naphthylethylamide derivative, shows improvement in potency compared to lead compound (compound **5h**, $IC_{50} = 2.3 \mu\text{M}$). The importance of an amide NH is demonstrated as the *N*-methyl derivative has significantly attenuated potency (compound **21**, $IC_{50} = 22.6 \mu\text{M}$; compound **5h**, $IC_{50} = 2.3 \mu\text{M}$). 5-Amino group resulted in an even more potent inhibitor **24** with an IC_{50} value of $0.56 \mu\text{M}$. However, incorporation of a polar acetamide derivative afforded a less potent derivative (compound **25**, $IC_{50} = 2.6 \mu\text{M}$).

To obtain molecular insights into the ligand-binding site interactions responsible for the inhibitory potency of compound **24**, the X-ray structure of PLpro complexed with **24** was determined previously to 2.5\AA resolution.^{13, 23} Comparison of the apoenzyme SARS-CoV PLpro structure to the inhibitor **24**-complexed structure reveals significant conformational differences between these structures.²³ Based upon this molecular insight, we further modified the substituents on the benzamide ring. Particularly interesting is the fact that the amine group in **24** is positioned at the opening of the cleft where it appears to come within hydrogen bonding distance to the hydroxyl of Tyr269. Furthermore, there are a number of water molecules present (see Figure 2) that occupy the pocket accommodating the (*R*)-methyl substituent of **24**. This suggested the potential for extending the methyl branch further into the pocket through the addition of polar substituents. As shown in Table 4, we incorporated a dimethyl group in place of the (*R*)-methyl substituent, however the corresponding inhibitor showed a reduction in potency for SARS PLpro (compound **29**, $IC_{50} = 11.1 \mu\text{M}$). Based upon the X-ray structure, we then incorporated 5-methylamine substituents on the benzamide ring. The resulting compound **2** showed a slight improvement in inhibitory potency (compound **2**, $IC_{50} = 0.46 \mu\text{M}$) and antiviral activity ($EC_{50} = 12.5 \mu\text{M}$) as shown in Table 5. The addition of a methyl group to the amine group of **2**, provided compound **49** which showed slightly decreased enzyme activity ($IC_{50} = 1.3 \mu\text{M}$) but significantly improved antiviral potency ($EC_{50} = 2.5 \mu\text{M}$). These results illustrate the importance of testing compounds not only for their ability to inhibit the purified protein, but also to assess their effects on cell viability and inhibition of viral replication in a cell-based assay.

To obtain molecular insights into the active site interactions leading to improved inhibitory potency, we created an energy-minimized model of **2** in the **24**-inhibited SARS-CoV PLpro active site (Figure 2B). The model reveals that the 5-methylamine substituent of inhibitor **2** may be involved in hydrogen bonding with the side chain of residues Gln270 and Tyr269.

Similar to the crystal structure conformation of compound **24**, compound **2** appears to be anchored in the site by two effective hydrogen bonds made between the carboxamide group and residue Asp165 and Gln 270. The three conserved water molecules found in both the complex crystal structure of compound **24**-bound protein and the crystal structure of the apo enzyme are retained for modelling studies and are shown as red dots in the P5 binding pocket (see Figure 2B). In docking studies, these water molecules are necessary for obtaining the crystal bound orientation of these compounds which positions the naphthyl ring of the inhibitor to be flipped upwards holding the loop (shown in cyan, Figure 2A). In the absence of these three waters, the naphthyl ring tends to occupy the P5 pocket, shown in green, Figure 2A.

To better quantitate and understand the contributions of the inhibitor substituents to the inhibitory potency, we also conducted an extensive Quantitative Structural Activity Relationship (QSAR) analysis. QSAR studies are often employed as a standard method to determine valuable information for designing novel and potent inhibitors. An alternative approach to labor-intensive chemical synthesis is to develop a theory that quantitatively relates variations in biological activity to changes in molecular descriptors for each compound. The goal of our computational study was to develop a robust QSAR model that can predict and differentiate inhibition values of this series of inhibitors against SARS-CoV PLpro. Partial least squares (PLS) methodology was used for the 3D-QSAR analyses. The CoMSIA descriptors were used as independent variables and percent inhibition values at 100 μ M were used as dependent variables in PLS regression analyses to derive the models. The predictive value of the models were evaluated by leave-one-out (LOO) cross-validation. To assist ligand-based structure design efforts, we used docking in conjunction with 3D-QSAR (CoMSIA) to investigate the SAR of 46 inhibitors with considerable structural diversity and a wide range of bioactivity against the SARS-CoV PLpro.

The crystal structures of the apo protein (PDB id: 2fe8)¹¹ and the inhibitor **24**-bound form (PDB id: 3e9s)¹³ were carefully studied, and it was determined that three water molecules are conserved in the active sites of both the structures; two are buried deep in the P5 pocket and one between residues Lys158 and Glu168. Apart from these three conserved water molecules, two additional water molecules are located at the ridge by the P5 pocket in the inhibitor-bound form of the protein. As previously mentioned, by conducting extensive analyses both with and without water molecules bound to the structures, we determined that retaining the three conserved water molecules made a substantial difference in replicating the crystal structure binding geometry of compound **24** in docking studies. When docking was performed in the absence of water molecules in the P5 pocket, the study suggested that the naphthyl rings prefer to flip downward and probably find lower energy conformations in this pocket as shown in Figure 2A. In the inhibitor **24**-bound crystal structure, two of the conserved water molecules hinder placement of the naphthyl rings in the P5 pocket and thereby flip the rings upwards. This position of the naphthyl rings fits nicely in the hydrophobic pocket and forms favorable interactions with the flexible loop residues. The five water molecules mentioned above are clearly shown in Figure 2B and were retained for the docking procedure prior to CoMSIA²⁴ model generation. In Figure 2B, the superimposition of the naphthyl rings of modeled compound **2** (green) and x-ray structure bound orientation of compound **24** (cyan) is clearly shown as obtained in the presence of the conserved water molecules.

Using the binding conformation of inhibitor **24** from the crystal structure as a template, 45 other inhibitors were docked. The docked geometry of these 45 inhibitors aligned very well with the binding geometry of compound **24** in the crystal structure. A predictive 3D-QSAR model was derived from the alignment of the docked conformations of the inhibitors as extracted directly from the 3D coordinates of the docked complexes. A successful CoMSIA

model was built with a cross-validated q^2 of 0.678 and bootstrap R^2 of 0.984. It is imperative to mention here that without the inclusion of at least the three conserved water molecules, the docking geometry of the inhibitors does not align with the crystal structure (as shown in Figure 2A). In the absence of these water molecules, the wrong ligand conformation is generated where the naphthyl ring is flipped into the P5 pocket, consequently resulting in an SAR with no correlation.

The CoMSIA model at six components gave a cross-validated q^2 of 0.678, r^2 of 0.984, F of 302.2 and a mean standard error estimate of 4.72. The high r^2 of 0.984 illustrates that the physicochemical descriptors chosen were appropriate to describe the binding interactions mode of the various inhibitors with the PLpro active site. The plot shown in Figure 3 shows the correlation between the experimental percent inhibition values of 41 compounds and the inhibition percentages predicted by the CoMSIA model. The contour maps generated, shown in Figures 4A–C, were mapped back to the topology of the active site to reveal that electrostatic, hydrophobic, and steric fields were in accordance with the distribution of the binding site residues. These contour maps should prove to be helpful in determining the incorporation of functional groups for the inhibitors that can extensively interact with specific binding pocket residues. We conclude that this robust 3D-QSAR model built using CoMSIA can be used as a reliable guide for future structure-based drug design efforts.

Conclusion

In summary, a series of novel inhibitors of SARS-CoV PLpro has been designed, synthesized and evaluated in enzyme inhibitory and antiviral assay. Initial lead compound **1** was discovered via high-throughput screening. This racemic compound has shown enzyme IC_{50} value of 20 μ M. The stereochemical preference for the *R*-isomer was established through synthesis and evaluation of optically pure inhibitors, and kinetic studies showed that the optically pure lead inhibitor is a reversible inhibitor of SARS-CoV-PLpro enzyme. In the absence of any structural information, initially our structure-activity-relationship studies and systematic modification guided by molecular modeling studies provided potent inhibitor **24**. This inhibitor displayed enzyme inhibitory activity of 560 nM and antiviral EC_{50} value of 14.5 μ M in SARS-CoV infected Vero E6 cells. A protein-ligand X-ray structure of **24**-bound SARS-CoV PLpro provided detailed molecular interaction in the active site of PLpro enzyme. Based upon the X-ray structural information, our structure-based design led to identification of potent inhibitors **2** and **49**. Inhibitor **2** has shown potent enzyme inhibitor activity of 460 nM and antiviral EC_{50} value of 12.5 μ M against SARS. Interestingly, the corresponding methylamine derivative **49** (enzyme IC_{50} = 1.3 μ M) has shown most potent antiviral activity against SARS (EC_{50} = 2.5 μ M). To obtain molecular insight into the binding properties of **2** and its derivative, we have created active model based upon the X-ray structure of **24**-bound SARS PLpro. It appears that the methylamine functionality is within proximity to hydrogen bond with the side chain residues of Gln270 and Tyr269. We have also carried out computational docking studies and generated predictive 3D-QSAR model for SARS-CoV PLpro. Further design of reversible SARS-CoV PLpro inhibitors is currently underway in our laboratory.

Experimental Section

Chemistry

1 H-NMR and 13 C-NMR spectra were recorded on Varian Oxford 300 and Bruker Avance 400 spectrometers. Optical rotations were recorded on Perkin-Elmer 341 polarimeter. Anhydrous solvent was obtained as follows: dichloromethane by distillation from CaH_2 , THF by distillation from Na and benzophenone. All other solvents were reagent grade. Column chromatography was performed with Whatman 240–400 mesh silica gel under low

pressure of 3–5 psi. TLC was carried out with E. Merck silica gel 60-F-254 plates. Purity of all test compounds was determined by HRMS and HPLC analysis on an Agilent 1100 unit in two different solvent systems. All test compounds showed $\geq 95\%$ purity.

General procedure for coupling reaction of naphthylethylamine and benzoic acid derivative

2-Methyl-*N*-[(*R*)-1-(1-naphthyl)ethyl]benzamide (5h)—To a solution of *o*-toluic acid (16.2 mg, 0.12 mmol), *N*-(3-dimethylaminopropyl)-*N'*-ethylcarbodiimide hydrochloride (EDCI) (29.1 mg, 0.15 mmol) and 1-hydroxybenzotriazole hydrate (HOBT) (20.5 mg, 0.15 mmol) in dry-CH₂Cl₂ was added a solution of (*R*)-(+)-1-(1-naphthyl)ethylamine **18** (20 mg, 0.12 mmol) and diisopropylethylamine (81.4 μ L, 0.47 mmol) in dry-CH₂Cl₂ at 0 °C under argon atmosphere and it was allowed to stir for 15 h at 23 °C. The reaction mixture was quenched with water and extracted with CH₂Cl₂. The organic layers were dried over Na₂SO₄ and concentrated under reduced pressure. The residue was purified by silica gel column chromatography to furnish compound **5I** (33 mg, 98%) as a white solid, $R_f = 0.34$ (hexane: EtOAc = 3:1), $[\alpha]_D^{20} -50.0$ ($c=1$, CHCl₃); ¹H NMR (400 MHz, CDCl₃): δ 8.24 (d, 1H, $J = 8.5$ Hz), 7.89 (d, 1H, $J = 8.0$ Hz), 7.82 (d, 1H, $J = 8.0$ Hz), 7.60–7.51 (m, 3H), 7.46 (dd, 1H, $J = 7.6$ and 7.7 Hz), 7.27–7.24 (m, 2H), 7.17 (d, 1H, $J = 7.7$ Hz), 7.11 (dd, 1H, $J = 7.6$ and 8.0 Hz), 6.15–6.07 (m, 2H), 2.44 (s, 3H), 1.79 (d, 3H, $J = 6.4$ Hz); ¹³C NMR (100 MHz, CDCl₃): δ 168.9, 137.9, 136.3, 136.0, 133.9, 131.1, 130.9, 129.7, 128.7, 128.4, 126.5, 126.5, 129.5, 125.6, 125.1, 123.5, 122.5, 44.8, 20.5, 19.7. MS (EI): m/z 289.20 [M]⁺; HRMS (EI), calcd for C₂₀H₁₉NO 289.1467, found [M]⁺ 289.1468.

3-Methyl-*N*-[(*R*)-1-(2-naphthyl)ethyl]benzamide (5a)—The title compound was obtained as described in the general procedure in 92% yield (white solid). $R_f = 0.35$ (hexane: EtOAc = 3:1), $[\alpha]_D^{20} +39.5$ ($c=1$, CHCl₃); ¹H NMR (300 MHz, CDCl₃): δ 7.83–7.79 (m, 4H), 7.60–7.44 (m, 5H), 7.27 (d, 2H, $J = 5.4$ Hz), 6.51 (d, 1H, $J = 6.9$ Hz), 5.53–5.44 (m, 1H), 2.35 (s, 3H), 1.67 (d, 3H, $J = 6.6$ Hz); ¹³C NMR (75 MHz, CDCl₃): δ 166.8, 140.5, 138.3, 134.5, 133.3, 132.7, 132.2, 128.5, 128.4, 127.9, 127.6, 127.6, 126.2, 125.8, 124.8, 124.6, 123.9, 49.1, 21.5, 21.3. MS (EI): m/z 289.15 [M]⁺; HRMS (EI), calcd for C₂₀H₁₉NO 289.1467, found [M]⁺ 289.1468.

4-Methyl-*N*-[(*R*)-1-(2-naphthyl)ethyl]benzamide (5b)—The title compound was obtained as described in the general procedure in >99% yield (white solid). $R_f = 0.32$ (hexane: EtOAc = 3:1), $[\alpha]_D^{20} +19.7$ ($c=1$, CHCl₃); ¹H NMR (300 MHz, CDCl₃): δ 7.82–7.79 (m, 4H), 7.68 (d, 2H, $J = 8.1$ Hz), 7.50–7.42 (m, 3H), 7.17 (d, 2H, $J = 7.5$ Hz), 6.59 (d, 1H, $J = 6.9$ Hz), 5.52–5.42 (m, 1H), 2.36 (s, 3H), 1.64 (d, 3H, $J = 6.9$ Hz); ¹³C NMR (75 MHz, CDCl₃): δ 166.5, 141.8, 140.6, 133.3, 132.7, 131.6, 129.1, 128.5, 127.9, 127.6, 126.9, 126.2, 125.8, 124.8, 124.6, 49.1, 21.6, 21.4. MS (EI): m/z 289.10 [M]⁺; HRMS (EI), calcd for C₂₀H₁₉NO 289.1467, found [M]⁺ 289.1469.

2-Methoxy-*N*-[(*R*)-1-(2-naphthyl)ethyl]benzamide (5c)—The title compound was obtained as described in the general procedure in >99% yield (white solid). $R_f = 0.23$ (hexane: EtOAc = 3:1), $[\alpha]_D^{20} -30.7$ ($c=1$, CHCl₃); ¹H NMR (300 MHz, CDCl₃): δ 8.28 (d, 1H, $J = 7.8$ Hz), 8.22 (dd, 1H, $J = 1.8$ and 8.1 Hz), 7.52 (dd, 1H, $J = 1.8$ and 8.7 Hz), 7.49–7.40 (m, 3H), 7.07 (t, 1H, $J = 7.7$ Hz), 6.95 (d, 1H, $J = 9.0$ Hz), 5.57–5.47 (m, 1H), 3.92 (s, 3H), 1.67 (d, 3H, $J = 6.3$ Hz); ¹³C NMR (75 MHz, CDCl₃): δ 164.4, 157.5, 141.2, 133.4, 132.7, 132.6, 132.3, 128.4, 127.8, 127.6, 126.1, 125.7, 124.7, 124.4, 121.6, 121.3, 111.3, 55.9, 49.1, 22.3. MS (EI): m/z 305.15 [M]⁺; HRMS (EI), calcd for C₂₀H₁₉NO₂ 305.1416, found [M]⁺ 305.1414.

3-Methoxy-*N*-[(*R*)-1-(2-naphthyl)ethyl]benzamide (5d)—The title compound was obtained as described in the general procedure in >99% yield (white solid). $R_f = 0.24$ (hexane: EtOAc = 3:1), $[\alpha]_D^{20} +50.0$ ($c=1$, CHCl₃); ¹H NMR (300 MHz, CDCl₃): δ 7.82-7.79 (m, 4H), 7.50-7.44 (m, 3H), 7.38-7.38 (m, 1H), 7.31-7.27 (m, 2H), 7.03-6.97 (m, 1H), 6.57 (d, 1H, $J = 7.8$ Hz), 5.51-5.42 (m, 1H), 3.79 (s, 3H), 1.65 (d, 3H, $J = 7.2$ Hz); ¹³C NMR (75 MHz, CDCl₃): δ 166.4, 159.8, 140.5, 136.0, 133.3, 132.7, 129.5, 128.5, 127.9, 127.6, 126.2, 125.9, 124.7, 124.6, 118.6, 117.7, 112.4, 55.4, 49.3, 21.5. MS (EI): m/z 305.20 [M]⁺; HRMS (EI), calcd for C₂₀H₁₉NO₂ 305.1416, found [M]⁺ 305.1417.

4-Methoxy-*N*-[(*R*)-1-(2-naphthyl)ethyl]benzamide (5e)—The title compound was obtained as described in the general procedure in >99% yield (white solid). $R_f = 0.20$ (hexane: EtOAc = 3:1), $[\alpha]_D^{20} +3.0$ ($c=1$, CHCl₃); ¹H NMR (300 MHz, CDCl₃): δ 7.81-7.73 (m, 6H), 7.49-7.41 (m, 3H), 6.85 (d, 2H, $J = 8.7$ Hz), 6.58 (d, 1H, $J = 7.8$ Hz), 5.50-5.40 (m, 1H), 3.79 (s, 3H), 1.63 (d, 3H, $J = 6.9$ Hz); ¹³C NMR (75 MHz, CDCl₃): δ 166.1, 162.1, 140.7, 133.3, 132.7, 128.7, 128.4, 127.8, 127.5, 126.7, 126.1, 125.8, 124.8, 124.5, 113.6, 55.3, 49.1, 21.6. MS (EI): m/z 305.15 [M]⁺; HRMS (EI), calcd for C₂₀H₁₉NO₂ 305.1416, found [M]⁺ 305.1419.

2,6-dimethyl-*N*-[(*R*)-1-(2-naphthyl)ethyl]benzamide (5f)—The title compound was obtained as described in the general procedure in 94% yield (white solid). $R_f = 0.26$ (hexane: EtOAc = 3:1), $[\alpha]_D^{20} +32.9$ ($c=1$, CHCl₃); ¹H NMR (300 MHz, CDCl₃): δ 7.82-7.77 (m, 4H), 7.49-7.43 (m, 3H), 7.13 (dd, 1H, $J = 7.2$ and 8.1 Hz), 6.98 (d, 2H, $J = 7.5$ Hz), 6.17 (d, 1H, $J = 8.1$ Hz), 5.56-5.46 (m, 1H), 2.27 (s, 3H), 1.64 (d, 3H, $J = 6.3$ Hz); ¹³C NMR (75 MHz, CDCl₃): δ 169.3, 140.1, 137.5, 134.1, 133.2, 132.7, 128.6, 128.4, 127.8, 127.5, 127.4, 126.2, 125.9, 124.8, 124.6, 48.6, 21.4, 19.0. MS (EI): m/z 303.05 [M]⁺; HRMS (EI), calcd for C₂₁H₂₁NO 303.1623, found [M]⁺ 303.1624.

2-Hydroxy-*N*-[(*R*)-1-(2-naphthyl)ethyl]benzamide (5g)—The title compound was obtained as described in the general procedure in 97% yield (white solid). $R_f = 0.49$ (hexane: EtOAc = 3:1), $[\alpha]_D^{20} +68.3$ ($c=1$, CHCl₃); ¹H NMR (300 MHz, CDCl₃): δ 12.39 (s, 1H), 7.85-7.80 (m, 4H), 7.51-7.33 (m, 5H), 6.97 (d, 1H, $J = 8.1$ Hz), 6.81-6.76 (m, 2H), 5.49-5.39 (m, 1H), 1.67 (d, 3H, $J = 7.2$ Hz); ¹³C NMR (75 MHz, CDCl₃): δ 169.2, 161.5, 139.8, 134.2, 133.2, 132.7, 128.6, 127.8, 127.6, 126.3, 126.0, 125.4, 124.5, 124.5, 118.6, 118.5, 114.1, 49.1, 21.5. MS (EI): m/z 291.10 [M]⁺; HRMS (EI), calcd for C₁₉H₁₇NO₂ 291.1259, found [M]⁺ 291.1261.

2-Methyl-5-nitro-*N*-[(*R*)-1-(1-naphthyl)ethyl]benzamide (5i)—The title compound was obtained as described in the general procedure in 95% yield (white solid). $R_f = 0.24$ (hexane: EtOAc = 3:1), $[\alpha]_D^{20} -53.0$ ($c=1$, CHCl₃); ¹H NMR (300 MHz, CDCl₃): δ 8.18 (d, 1H, $J = 8.1$ Hz), 8.11-8.06 (m, 2H), 7.87 (d, 1H, $J = 8.0$ Hz), 7.81 (d, 1H, $J = 8.0$ Hz), 7.60-7.43 (m, 4H), 7.32 (d, 1H, $J = 8.4$ Hz), 6.13-6.10 (bm, 2H), 2.49 (s, 3H), 1.80 (d, 3H, $J = 6.3$ Hz); ¹³C NMR (75 MHz, CDCl₃): δ 166.5, 144.3, 137.8, 137.3, 133.8, 131.9, 131.1, 128.9, 128.8, 126.7, 126.1, 125.2, 124.4, 123.2, 122.7, 122.6, 121.6, 45.2, 20.5, 20.0. MS (EI): m/z 334.20 [M]⁺; HRMS (EI), calcd for C₂₀H₁₈N₂O₃ 334.1317, found [M]⁺ 334.1323.

4-*N*-*TERT*-Butoxycarbonylaminobenzoic acid (7)—To a solution of 4-aminobenzoic acid **6** (520 mg, 3.8 mmol) in dioxane/H₂O (2:1) (13 mL) was added triethylamine (0.79 mL, 5.7 mmol) and Boc₂O (1.31 mL, 5.7 mmol) at 23 °C and it was allowed to stir for 48 h at same temperature. The solvent was removed under reduced pressure, and 3M HCl (5 mL) was added dropwise to the residue at 0 °C. A precipitate was obtained, collected, washed with water, and dried to give corresponding acid **7** (836 mg, 93%) as slightly yellow solid, $R_f = 0.78$ (CH₂Cl₂: MeOH = 9:1), ¹H NMR (400 MHz, CDCl₃): δ 9.25 (brs, 1H), 7.91 (d,

2H, $J = 8.7$ Hz), 7.50 (d, 2H, $J = 8.7$ Hz), 1.51 (s, 9H); ^{13}C NMR (100 MHz, CDCl_3): δ 169.7, 154.8, 131.8, 125.3, 118.6, 118.5, 81.3, 28.6. MS (EI): m/z 237.10 $[\text{M}]^+$; HRMS (EI), calcd for $\text{C}_{12}\text{H}_{15}\text{NO}_4$ 237.1001, found $[\text{M}]^+$ 237.1004.

4-*N*-TERT-Butoxycarbonylamino-*N*-[(*R*)-1-(2-naphthyl)ethyl]benzamide (8)—

The title compound was obtained as described in the general procedure in 60% yield (white solid). $R_f = 0.76$ (CH_2Cl_2 : MeOH = 9:1), $[\alpha]_D^{20} -91.6$ ($c=1$, CHCl_3 : MeOH = 1:1); ^1H NMR (300 MHz, CDCl_3): δ 7.77-7.72 (m, 6H), 7.48-7.37 (m, 5H), 5.40-5.33 (m, 1H), 1.60 (d, 3H, $J = 6.9$ Hz), 1.47 (s, 9H). MS (EI): m/z 390.05 $[\text{M}]^+$; HRMS (EI), calcd for $\text{C}_{24}\text{H}_{26}\text{N}_2\text{O}_3$ 390.1943, found $[\text{M}]^+$ 390.1942.

4-amino-*N*-[(*R*)-1-(2-naphthyl)ethyl]benzamide (9)—To a solution of Boc **8** (60 mg, 0.15 mmol) in CH_2Cl_2 (4 mL) was added dropwise trifluoroacetic acid (0.6 mL) at 23 °C and it was allowed to stir for 2 h at same temperature. The reaction was concentrated under reduced pressure and the residue was treated with saturated NaHCO_3 solution. The mixture was extracted with CH_2Cl_2 . The organic layers were dried over Na_2SO_4 and concentrated under reduced pressure. The residue was purified by silica gel column chromatography to give compound **9** (44 mg, 99%) as a white solid, $R_f = 0.60$ (CH_2Cl_2 : MeOH = 9:1), $[\alpha]_D^{20} -58.0$ ($c=1$, CHCl_3 : MeOH = 4:1); ^1H NMR (300 MHz, CDCl_3): δ 7.82-7.80 (m, 4H), 7.60 (d, 2H, $J = 8.1$ Hz), 7.50-7.41 (m, 3H), 6.63 (d, 2H, $J = 8.7$ Hz), 6.23 (d, 1H, $J = 6.9$ Hz), 5.52-5.42 (m, 1H), 1.66 (d, 3H, $J = 7.2$ Hz). MS (EI): m/z 290.15 $[\text{M}]^+$; HRMS (EI), calcd for $\text{C}_{19}\text{H}_{18}\text{N}_2\text{O}$ 290.1419, found $[\text{M}]^+$ 290.1424.

1-(2-Naphthyl)propanone (12)—To a solution of propionyl chloride **11** (5.1 g, 55 mmol) and aluminium chloride (7.7 g, 58 mmol) in 1,2-dichloroethane (16 mL) was added dropwise a solution of naphthalene **10** (7.9 g, 62 mmol) in 1,2-dichloroethane (16 mL) over 3 h at 35 °C and it was allowed to stir for 1 h. The reaction was added 3M HCl solution at 0 °C and then separate a white solid. The filtrate was washed with water. The organic layer was dried over Na_2SO_4 and concentrated under reduced pressure. The residue was purified by silica gel column chromatography to furnish compound **12** (9.9 g, 98%) as a colorless oil, $R_f = 0.56$ (hexane: EtOAc = 9:1), ^1H NMR (300 MHz, CDCl_3): δ 8.58 (d, 1H, $J = 8.7$ Hz), 7.94 (d, 1H, $J = 8.1$ Hz), 7.86-7.80 (m, 2H), 7.59-7.42 (m, 3H), 3.04 (q, 2H, $J = 6.9$ Hz), 1.27 (t, 3H, $J = 6.9$ Hz); ^{13}C NMR (75 MHz, CDCl_3): δ 205.2, 136.0, 133.8, 132.2, 130.0, 128.3, 127.7, 127.1, 126.3, 125.7, 124.3, 35.2, 8.56. MS (EI): m/z 184.15 $[\text{M}]^+$; HRMS (EI), calcd for $\text{C}_{13}\text{H}_{12}\text{O}$ 184.0888, found $[\text{M}]^+$ 184.0890.

2-Methyl-*N*-[1-(2-naphthyl)propyl]benzamide (14)—To a solution of ketone **12** (2.1 g, 11.4 mmol) in MeOH (50 mL) was added ammonium acetate (8.8 g, 0.11 mol) and NaBH_3CN (528 mg, 8.0 mmol) at 23 °C and was stirred for 24 h. Conc. HCl was added until pH <2, and the solvent was removed under reduced pressure. The residue was taken up in water (15 mL) and extracted once with Et_2O . The aqueous layer was brought to pH >12 with solid KOH and extracted with CH_2Cl_2 . The organic layers were dried over Na_2SO_4 and concentrated under reduced pressure to give amine **13** as crude compound, MS (EI): m/z 185.20 $[\text{M}]^+$; HRMS (EI), calcd for $\text{C}_{13}\text{H}_{15}\text{N}$ 185.1204, found $[\text{M}]^+$ 185.1206. Coupling reaction was used general procedure with amine **13** (50 mg, mmol) and *o*-toluic acid (37.5 mg, mmol) to give inhibitor **14** (21 mg, 2 steps 26%) as a white solid, $R_f = 0.25$ (hexane: EtOAc = 3:1), ^1H NMR (300 MHz, CDCl_3): δ 7.84-7.78 (m, 4H), 7.49-7.44 (m, 3H), 7.35-7.26 (m, 2H), 7.20-7.14 (m, 2H), 6.12 (d, 1H, $J = 8.4$ Hz), 5.28-5.20 (m, 1H), 2.39 (s, 3H), 2.04-1.95 (m, 2H), 0.99 (t, 3H, $J = 7.2$ Hz); ^{13}C NMR (75 MHz, CDCl_3): δ 169.4, 139.4, 136.6, 136.0, 133.3, 132.7, 130.9, 129.8, 128.5, 127.8, 127.6, 126.5, 126.2, 125.8, 125.7, 125.3, 124.7, 55.2, 29.1, 19.7, 10.9. MS (EI): m/z 303.25 $[\text{M}]^+$; HRMS (EI), calcd for $\text{C}_{21}\text{H}_{21}\text{NO}$ 303.1623, found $[\text{M}]^+$ 303.1624.

1-(2-Naphthyl)benzylamine (16)—To a solution of naphthylphenylketone **15** (600 mg, 2.6 mmol) in MeOH (15 mL) was added ammonium acetate (2 g, 25.9 mmol) and NaBH₃CN (120 mg, 1.9 mmol) at 23 °C and it was allowed to stir for 24 h. Conc. HCl was added until pH <2, and the solvent was removed under reduced pressure. The residue was taken up in water (4 mL) and extracted once with Et₂O. The aqueous layer was brought to pH >12 with solid KOH and extracted with CH₂Cl₂. The organic layers were dried over Na₂SO₄ and concentrated under reduced pressure to give amine **16** (48 mg, 8%) as crude compound, R_f = 0.53 (CH₂Cl₂: MeOH = 4:1), ¹H NMR (300 MHz, CDCl₃): δ 7.74-7.53 (m, 5H), 7.28-7.18 (m, 4H), 7.13-7.01 (m, 3H), 5.14 (s, 1H), 1.89 (bs, 1H); ¹³C NMR (75 MHz, CDCl₃): δ 145.2, 142.8, 133.3, 132.5, 130.0, 128.5, 128.2, 127.9, 127.6, 127.0, 126.0, 125.7, 125.6, 124.9, 59.7. MS (EI): *m/z* 233.30 [M]⁺; HRMS (EI), calcd for C₁₇H₁₅N 233.1204, found [M]⁺ 233.1205.

2-Methyl-N-[1-(2-naphthyl)benzyl]benzamide (17)—The title compound was obtained as described in the general procedure in 72% yield (white solid). R_f = 0.39 (hexane: EtOAc = 3:1), ¹H NMR (300 MHz, CDCl₃): δ 7.88-7.80 (m, 5H), 7.55-7.34 (m, 9H), 7.29-7.24 (m, 2H), 6.66 (d, 1H, *J* = 8.4 Hz), 6.57 (d, 1H, *J* = 8.4 Hz); ¹³C NMR (75 MHz, CDCl₃): δ 169.1, 141.3, 138.7, 136.3, 136.0, 133.2, 132.7, 131.1, 130.0, 128.7, 128.7, 128.6, 128.0, 127.6, 127.5, 126.6, 126.3, 126.1, 126.0, 125.7, 125.5, 57.3, 19.8. MS (EI): *m/z* 351.40 [M]⁺; HRMS (EI), calcd for C₂₅H₂₁NO 351.1623, found [M]⁺ 351.1618.

N-Methoxycarbonyl-(R)-(+)-1-(2-naphthyl)ethylamine (19)—To a solution of (*R*)-(+)-1-(2-naphthyl)ethylamine **18** (200 mg, 1.2 mmol) in a mixture (1:1) of dioxane and H₂O was added potassium carbonate (323 mg, 2.3 mmol) and methyl chloroformate (0.11 mL, 1.4 mmol) at 0 °C and it was allowed to stir for 1 h at 0 °C. The reaction was quenched with 10% HCl solution and extracted with EtOAc. The organic layers were dried over Na₂SO₄ and concentrated under reduced pressure. The residue was purified by silica gel column chromatography to furnish compound **19** (268 mg, >99%) as a colorless oil, R_f = 0.36 (hexane: EtOAc = 3:1), [α]_D²⁰ +96.8 (*c*=1, CHCl₃); ¹H NMR (300 MHz, CDCl₃): δ 7.82-7.74 (m, 4H), 7.50-7.40 (m, 3H), 5.14 (bm, 1H), 5.00 (bm, 1H), 3.66 (s, 3H), 1.54 (d, 3H, *J* = 6.9 Hz); ¹³C NMR (75 MHz, CDCl₃): δ 156.2, 140.9, 133.1, 132.5, 128.1, 127.7, 127.4, 125.9, 125.5, 124.2, 124.1, 51.8, 50.5, 22.0. MS (EI): *m/z* 229 [M]⁺; HRMS (EI), calcd for C₁₄H₁₅NO₂ 229.1103, found [M]⁺ 229.1103.

N-Methyl-(R)-(+)-1-(2-naphthyl)ethylamine (20)—To a suspension of lithium aluminum hydride (93 mg, 2.4 mmol) in THF (6 mL) was added dropwise a solution of carbamate **19** (268 mg, 1.2 mmol) in THF (1 mL) at 0 °C under argon atmosphere and it was allowed to stir for 1 h at reflux temperature. The reaction was quenched with 1M NaOH solution at 0 °C and the mixture was filtered through celite pad. The filtrate was concentrated under reduced pressure and the residue was purified by silica gel column chromatography to give amine **20** (186 mg, 86%) as a colorless oil, R_f = 0.21 (CH₂Cl₂: MeOH = 9:1), [α]_D²⁰ +58.0 (*c*=1, CHCl₃); ¹H NMR (300 MHz, CDCl₃): δ 7.83-7.80 (m, 3H), 7.73 (s, 1H), 7.49-7.40 (m, 3H), 3.81 (q, 1H, *J* = 6.6 Hz), 2.33 (s, 3H), 1.80 (bs, 1H), 1.43 (d, 3H, *J* = 6.6 Hz); ¹³C NMR (75 MHz, CDCl₃): δ 142.4, 133.2, 132.6, 128.0, 127.5, 127.4, 125.7, 125.3, 125.1, 124.6, 60.1, 34.3, 23.7. MS (EI): *m/z* 185.30 [M]⁺; HRMS (EI), calcd for C₁₃H₁₅N 185.1204, found [M]⁺ 185.1205.

2,N-Dimethyl-N-[(R)-1-(2-naphthyl)ethyl]benzamide (21)—The title compound was obtained as described in the general procedure in 87% yield (white solid). R_f = 0.26 (hexane: EtOAc = 3:1), [α]_D²⁰ +189.1 (*c*=1, CHCl₃); ¹H NMR (300 MHz, CDCl₃): δ 7.96-7.91 (m, 3.6H), 7.74-7.71 (m, 0.4H), 7.65-7.55 (m, 2.6H), 7.47-7.24 (m, 4.4H), 6.53 (q, 0.6H, *J* = 7.2 Hz), 5.11-5.08 (m, 0.4H), 3.04 (s, 0.7H), 2.97 (s, 0.4H), 2.54 (s, 2.6H), 2.43 (s, 2.3H), 1.82

(d, 2.1H, $J = 7.2$ Hz), 1.79-1.72 (m, 0.9H); ^{13}C NMR (75 MHz, CDCl_3): δ 171.5, 137.7, 137.0, 133.6, 133.1, 132.7, 130.3, 128.7, 128.3, 127.9, 127.5, 126.4, 126.2, 126.1, 126.0, 125.6, 125.5, 125.0, 124.6, 56.6, 56.3, 50.0, 30.4, 27.5, 18.9, 18.1, 15.3. MS (EI): m/z 303.30 $[\text{M}]^+$; HRMS (EI), calcd for $\text{C}_{21}\text{H}_{21}\text{NO}$ 303.1623, found $[\text{M}]^+$ 303.1627.

4-*N*-TERT-Butoxycarbonylamino-*N*-[(*R*)-1-(1-naphthyl)ethyl]benzamide (22)—

The title compound was obtained as described in the general procedure in >99% yield (white solid). $R_f = 0.73$ (CH_2Cl_2 : MeOH = 9:1), $[\alpha]^{20}_{\text{D}} -121.7$ ($c=1$, CHCl_3 : MeOH = 1:1); ^1H NMR (300 MHz, CDCl_3): δ 8.10 (d, 1H, $J = 8.1$ Hz), 7.80-7.73 (m, 2H), 7.59 (d, 2H, $J = 8.1$ Hz), 7.55 (d, 1H, $J = 7.5$ Hz), 7.49-7.34 (m, 2H), 7.42 (d, 1H, $J = 7.5$ Hz), 7.31 (d, 2H, $J = 8.1$ Hz), 7.04 (s, 1H), 6.52 (d, 2H, $J = 7.8$ Hz), 6.10-6.01 (m, 1H), 1.71 (d, 3H, $J = 6.6$ Hz), 1.47 (s, 9H); ^{13}C NMR (75 MHz, CDCl_3): δ 165.8, 152.4, 141.5, 138.3, 133.8, 131.1, 128.6, 128.3, 128.3, 127.9, 126.5, 125.7, 125.1, 123.4, 122.6, 117.6, 80.8, 45.1, 28.2, 20.7. MS (EI): m/z 390.25 $[\text{M}]^+$; HRMS (EI), calcd for $\text{C}_{24}\text{H}_{26}\text{N}_2\text{O}_3$ 390.1943, found $[\text{M}]^+$ 390.1947.

4-Amino-*N*-[(*R*)-1-(1-naphthyl)ethyl]benzamide (23)—The title compound was obtained as described in the compound **9** in 95% yield (slightly yellow solid). $R_f = 0.65$ (CH_2Cl_2 : MeOH = 4:1), $[\alpha]^{20}_{\text{D}} -137.8$ ($c=1$, CHCl_3 : MeOH = 4:1); ^1H NMR (300 MHz, CDCl_3): δ 8.15 (d, 1H, $J = 7.5$ Hz), 7.86-7.83 (m, 1H), 7.79 (d, 1H, $J = 8.1$ Hz), 7.58-7.42 (m, 6H), 6.59 (d, 1H, $J = 8.1$ Hz), 6.17 (d, 2H, $J = 7.5$ Hz), 6.13-6.03 (m, 1H), 1.74 (d, 3H, $J = 6.6$ Hz). MS (EI): m/z 290.35 $[\text{M}]^+$; HRMS (EI), calcd for $\text{C}_{19}\text{H}_{18}\text{N}_2\text{O}$ 290.1419, found $[\text{M}]^+$ 290.1422.

5-Amino-2-methyl-*N*-[(*R*)-1-(1-naphthyl)ethyl]benzamide (24)—To a stirred solution of nitro **5m** (37 mg, 0.11 mmol) in EtOAc/MeOH (1:1) (3 mL) was added 5% Pd-C (4 mg) and it was allowed to stir for 15 h at 23 °C under H_2 atmosphere. The reaction was filtered through celite pad and the filtrate was concentrated under reduced pressure. The residue was purified by silica gel column chromatography to furnish compound **24** (27 mg, 80%) as a white solid, $R_f = 0.29$ (hexane: EtOAc = 1:1), $[\alpha]^{20}_{\text{D}} -76.8$ ($c=1$, CHCl_3); ^1H NMR (300 MHz, CDCl_3): δ 8.20 (d, 1H, $J = 8.4$ Hz), 7.85 (d, 1H, $J = 8.0$ Hz), 7.78 (d, 1H, $J = 8.0$ Hz), 7.57-7.40 (m, 4H), 6.89 (d, 1H, $J = 8.0$ Hz), 6.70 (bd, 2H, $J = 13.5$ Hz), 6.10-6.07 (bm, 2H), 3.25 (bs, 2H), 2.27 (s, 3H), 1.73 (d, 3H, $J = 6.0$ Hz); ^{13}C NMR (75 MHz, CDCl_3): δ 169.0, 143.9, 138.0, 136.9, 133.8, 131.7, 131.1, 128.7, 128.3, 127.2, 126.5, 125.8, 125.1, 123.5, 122.5, 116.6, 113.3, 44.7, 20.5, 18.6. MS (EI): m/z 304.30 $[\text{M}]^+$.

5-*N*-Acetylamino-2-methyl-*N*-[(*R*)-1-(1-naphthyl)ethyl]benzamide (25)—To a stirred solution of amine **24** (14 mg, 0.05 mmol) in CH_2Cl_2 (0.5 mL) was added dropwise triethylamine (9.6 μL , 0.07 mmol) and acetic anhydride (5.2 μL , 0.06 mmol) at 0 °C and it was allowed to stir for 18 h at 23 °C. The reaction was quenched with saturated NH_4Cl solution and extracted with CH_2Cl_2 . The organic layers were dried over Na_2SO_4 and concentrated under reduced pressure. The residue was purified by silica gel column chromatography to furnish compound **25** (5.4 mg, 34%) as a white solid, $R_f = 0.60$ (CH_2Cl_2 : MeOH = 9:1), ^1H NMR (300 MHz, CDCl_3): δ 8.19 (d, 1H, $J = 8.1$ Hz), 7.85 (d, 1H, $J = 7.5$ Hz), 7.77 (d, 1H, $J = 8.1$ Hz), 7.56-7.39 (m, 4H), 7.35-7.32 (m, 2H), 7.04 (d, 1H, $J = 7.5$ Hz), 6.22 (d, 1H, $J = 8.1$ Hz), 6.12-6.03 (m, 1H), 2.33 (s, 3H), 2.05 (s, 3H), 1.74 (d, 3H, $J = 6.6$ Hz). MS (EI): m/z 346.30 $[\text{M}]^+$; HRMS (EI), calcd for $\text{C}_{22}\text{H}_{22}\text{N}_2\text{O}_2$ 346.1681, found $[\text{M}]^+$ 346.1682.

1-Methyl-1-(1-naphthyl)ethylamine (27)— $\text{CeCl}_3 \cdot 7\text{H}_2\text{O}$ (3.77 g, 10.1 mmol) was dried while stirring at 160 °C under reduced pressure for 3 h. Argon was added slowly, and the flask was cooled in an ice bath. THF (20 mL) was added and the suspension was stirred at 23 °C for 2 h. 1.5M methyl lithium in THF (6.7 mL, 10.1 mmol) was added below -50 °C.

The mixture was stirred for 30 min at $-78\text{ }^{\circ}\text{C}$ and a solution of 1-cyanonaphthalene **26** (500 mg, 3.3 mmol) in THF (2 mL) was added. Stirring at $23\text{ }^{\circ}\text{C}$ was continued for 2 h. Conc. NH_4OH (6.5 mL) was added at $-78\text{ }^{\circ}\text{C}$ and the mixture was warmed to $23\text{ }^{\circ}\text{C}$ and filtered with celite pad. The solid was washed with CH_2Cl_2 . The filtrate was extracted with CH_2Cl_2 and the organic layers were dried over Na_2SO_4 and concentrated under reduced pressure. The residue was taken up in toluene (10 mL) and stirred with 3% H_3PO_4 (10 mL) for 15 min. The toluene layer was extracted with water (x 2), and the combined water layers were washed with toluene and made basic with conc. NH_4OH solution. The mixture was extracted with CH_2Cl_2 and the organic layers were dried over Na_2SO_4 and concentrated under reduced pressure to furnish compound **27** (368 mg, 61%) as a colorless oil, $R_f = 0.25$ (CH_2Cl_2 : MeOH = 9:1), $^1\text{H NMR}$ (300 MHz, CDCl_3): δ 9.03 (d, 1H, $J = 9.0$ Hz), 7.98 (d, 1H, $J = 8.1$ Hz), 7.86 (d, 1H, $J = 8.4$ Hz), 7.71 (dd, 1H, $J = 1.2$ and 7.5 Hz), 7.65–7.48 (m, 3H), 1.89 (s, 6H); $^{13}\text{C NMR}$ (75 MHz, CDCl_3): δ 144.5, 135.0, 131.2, 129.2, 129.0, 128.1, 127.6, 124.9, 124.8, 122.8, 53.9, 33.3.

2-Methyl-5-nitro-*N*-[1-methyl-1-(1-naphthyl)ethyl]benzamide (28)—The title compound was obtained as described in the general procedure in 91% yield (white solid). $R_f = 0.26$ (hexane: EtOAc = 3:1), $^1\text{H NMR}$ (300 MHz, CDCl_3): δ 8.50 (d, 1H, $J = 8.1$ Hz), 8.07 (d, 1H, $J = 2.4$ Hz), 7.95 (dd, 1H, $J = 2.4$ and 8.4 Hz), 7.87 (d, 1H, $J = 8.4$ Hz), 7.76 (d, 1H, $J = 8.1$ Hz), 7.59 (d, 1H, $J = 7.5$ Hz), 7.54–7.39 (m, 3H), 7.17 (d, 1H, $J = 8.7$ Hz), 6.87 (bs, 1H), 2.24 (s, 3H), 1.95 (s, 6H); $^{13}\text{C NMR}$ (75 MHz, CDCl_3): δ 166.2, 145.3, 143.9, 140.6, 138.0, 134.9, 131.3, 131.4, 129.9, 129.8, 128.7, 125.3, 125.2, 125.1, 123.7, 123.7, 121.4, 57.5, 28.5, 19.5.

5-Amino-2-methyl-*N*-[1-methyl-1-(1-naphthyl)ethyl]benzamide (29)—The title compound was obtained as described for compound **24** in 75% yield (slightly yellow solid). $R_f = 0.18$ (hexane: EtOAc = 1:1), $^1\text{H NMR}$ (400 MHz, CDCl_3): δ 8.56 (d, 1H, $J = 8.7$ Hz), 7.88 (d, 1H, $J = 7.0$ Hz), 7.75 (d, 1H, $J = 8.1$ Hz), 7.65 (d, 1H, $J = 7.3$ Hz), 7.49–7.42 (m, 3H), 6.90 (d, 1H, $J = 8.0$ Hz), 6.60 (s, 1H), 6.53 (d, 1H, $J = 8.0$ Hz), 6.21 (s, 1H), 2.21 (s, 3H), 2.08 (s, 6H); $^{13}\text{C NMR}$ (100 MHz, CDCl_3): δ 169.1, 143.9, 141.2, 138.0, 135.0, 131.7, 130.2, 129.7, 128.7, 125.8, 125.2, 125.2, 125.0, 123.7, 116.3, 113.1, 57.5, 28.5, 18.6. MS (EI): m/z 318.45 $[\text{M}]^+$; HRMS (EI), calcd for $\text{C}_{21}\text{H}_{22}\text{N}_2\text{O}$ 318.1732, found $[\text{M}]^+$ 318.1729.

5-Iodo-2-methylbenzoic acid (31)— NaIO_4 (295 mg, 1.38 mmol) and KI (685 mg, 4.13 mmol) were added over 45 min slowly portionwise to stirred 95% H_2SO_4 (15 mL). Stirring was continued for 1 h at $25\text{--}30\text{ }^{\circ}\text{C}$ to give a dark brown iodinating solution.) at $25\text{--}30\text{ }^{\circ}\text{C}$. To a stirred solution of 2-toluic acid **30** (680 mg, 5 mmol) in 95% H_2SO_4 (5 mL), the iodinating solution was added dropwise over 45 min, while maintaining the temperature at $25\text{--}30\text{ }^{\circ}\text{C}$. Stirring was continued for 2 h and the iodination reaction was quenched by slowly pouring the final reaction mixture into stirred ice water. The mixture was extracted with AcOEt and dried over anhydrous Na_2SO_4 . The solvent was evaporated under reduced pressure and purification by silica gel flash column chromatography to afford compound **31** in 63% yield. $^1\text{H NMR}$ (400 MHz, CDCl_3): δ 8.38 (d, 1H, $J = 1.8$ Hz), 7.75 (dd, 1H, $J = 8.1$, 1.8 Hz), 7.02 (d, 1H, $J = 8.1$ Hz), 2.59 (s, 3H).

5-Iodo-2-methyl-*N*-[1-methyl-1-(1-naphthyl)ethyl]benzamide (32)—The title compound was obtained as described in the general procedure using DMF/ CH_2Cl_2 (1:1) as a solvent in 87% yield (white solid). $^1\text{H NMR}$ (400 MHz, CDCl_3): δ 8.20 (d, 1H, $J = 8.5$ Hz), 7.89 (d, 1H, $J = 8.0$ Hz), 7.83 (d, 1H, $J = 8.1$ Hz), 7.64–7.44 (m, 6H), 6.92 (d, 1H, $J = 7.8$ Hz), 6.12 (m, 1H), 5.94 (bd, 1H, $J = 8.3$ Hz), 2.36 (s, 3H), 1.80 (d, 3H, $J = 6.7$ Hz); $^{13}\text{C NMR}$ (100 MHz, CDCl_3): δ 167.1, 138.6, 138.4, 137.6, 135.6, 135.0, 133.9, 132.7, 131.1,

128.8, 128.6, 126.6, 125.9, 125.1, 123.3, 122.6, 90.0, 44.9, 20.5, 19.3. MS (ESI): m/z 438.0 [M + Na]⁺; HRMS (ESI), calcd for C₂₀H₁₈INONa 438.0331; found [M + Na]⁺ 438.0333.

5-Cyano-2-methyl-N-[1-methyl-1-(1-naphthyl)ethyl]benzamide (33)—Compound **32** (29 mg, 0.07 mmol) was dissolved in dry DMF (2 mL). CuCN (62 mg, 0.7 mmol) and a crystal of KCN were added. The mixture was flushed with nitrogen and stirred at 80 °C for 1 h then 130 °C for 10 h. CuCN (62 mg, 0.7 mmol) was added again. The mixture was flushed with nitrogen and stirred at 130 °C for 6 h. After this time, NH₄OH solution was poured into reaction mixture, and the mixture was extracted with AcOEt and dried over anhydrous Na₂SO₄. The solvent was evaporated under reduced pressure and purification by silica gel flash column chromatography to afford compound **33** in 78% yield as a white solid. ¹H NMR (400 MHz, CDCl₃): δ 8.19 (d, 1H, *J* = 8.4 Hz), 7.87 (d, 1H, *J* = 8.3 Hz), 7.84 (d, 1H, *J* = 8.2 Hz), 7.63–7.44 (m, 6H), 7.29 (d, 1H, *J* = 7.8 Hz), 6.12 (m, 1H), 6.08–5.99 (bs, 1H), 2.48 (s, 3H), 1.81 (d, 3H, *J* = 6.6 Hz); ¹³C NMR (100 MHz, CDCl₃): δ 166.6, 141.9, 137.4, 137.2, 133.9, 133.0, 131.8, 131.0, 130.1, 128.9, 128.7, 126.7, 126.0, 125.1, 123.1, 122.6, 118.1, 109.7, 45.0, 20.4, 20.1. MS (EI): m/z 314.10 [M]⁺; HRMS (EI), calcd for C₂₁H₁₈N₂O 314.1419; found [M]⁺ 314.1424.

2-Methyl-5-nitrobenzoic acid methyl ester (35)—To a stirring MeOH (4 mL) in a roundbottom flask was added dropwise thionyl chloride (0.24 mL, 3.3 mmol) at 0 °C. The mixture was added 2-methyl-5-nitrobenzoic acid **34** (300 mg, 1.7 mmol) at 0 °C and it was allowed to stir for 4 h at reflux temperature. The reaction was concentrated under reduced pressure and the residue was purified by silica gel column chromatography to give corresponding compound **35** (320 mg, 99%) as a colorless oil, *R_f* = 0.85 (hexane: EtOAc = 1:1), ¹H NMR (400 MHz, CDCl₃): δ 8.52 (s, 1H), 8.05 (s, 1H), 7.30 (s, 1H), 3.83 (s, 3H), 2.56 (s, 3H); ¹³C NMR (100 MHz, CDCl₃): δ 165.4, 147.6, 145.6, 132.5, 130.1, 125.8, 125.3, 52.1, 21.5. MS (EI): m/z 195 [M]⁺; HRMS (EI), calcd for C₉H₉NO₄ 195.0532, found [M]⁺ 195.0539.

2-Bromomethyl-5-nitrobenzoic acid methyl ester (36)—Compound **35** (100 mg, 0.53 mmol) was dissolved in CCl₄ (4 mL) followed by addition of NBS (100 mg, 0.58 mmol) and a catalytic amount of benzoyl peroxide. The mixture was stirred at reflux for 24 h. Another portion, of dibenzoyl peroxide (40 mg, 0.23 mmol) was added then the mixture was stirred and heated at reflux for another 10 h. The mixture was allowed to cool to 23 °C and was filtered. The filtrate was washed with NaHCO₃, dried over Na₂SO₄ and the solvent evaporated in vacuo. The residue was purified by silica gel column chromatography to afford compound **36** in 89% yield. ¹H NMR (400 MHz, CDCl₃): δ 8.81 (d, 1H, *J* = 2.5 Hz), 8.33 (dd, 1H, *J* = 8.5, 2.5 Hz), 7.68 (d, 1H, 8.5 Hz), 5.00 (s, 2H), 4.01 (s, 3H).

2-Methoxymethyl-5-nitrobenzoic acid methyl ester (37)—NaH (44 mg, 1.1 mmol) was added to a round-bottomed flask containing methanol (2 mL) at 0 °C. The sodium methoxide solution was added to a cold solution of compound **36** (60 mg, 0.22 mmol) in methanol (2 mL) at 0 °C. The resulting solution was stirred at 50 °C for 4 h. After this time, NH₄Cl solution was poured into reaction mixture at 0 °C, and the mixture was extracted with AcOEt and dried over anhydrous Na₂SO₄. The solvent was evaporated under reduced pressure and purification by silica gel flash column chromatography to afford corresponding compound **37** in 72% yield. ¹H NMR (400 MHz, CDCl₃): δ 8.82 (d, 1H, *J* = 2.4 Hz), 8.38 (dd, 1H, *J* = 8.7, 2.4 Hz), 7.94 (d, 1H, 8.7 Hz), 4.94 (s, 2H), 3.96 (s, 3H), 3.53 (s, 3H).

2-Methoxymethyl-5-nitrobenzoic acid (38)—To a stirring solution of compound **37** (36 mg, 0.75 mmol) in THF: H₂O mixture (5 mL:1 mL) at 0 °C was added solid LiOH·H₂O (120 mg, 5 mmol), and the resulting solution was stirred at ambient temperature for 1.5 h.

After this period, the reaction mixture was evaporated until 1 mL and the mixture was extracted with toluene to remove organic impurities. The aqueous layer was cooled to 0 °C, acidified with 25% aqueous citric acid until pH 3–4, extracted with AcOEt, and dried over anhydrous Na₂SO₄. The solvent was evaporated and purification by silica gel flash column chromatography to furnish compound **37** in 90% yield. ¹H NMR (400 MHz, CD₃OD and CDCl₃): δ 8.73 (d, 1H, *J* = 2.4 Hz), 8.26 (dd, 1H, *J* = 8.6, 2.4 Hz), 7.80 (d, 1 H, 8.6 Hz), 4.88 (s, 2H), 3.43 (s, 3H).

2-Methoxymethyl-5-nitro-N-[1-methyl-1-(1-naphthyl)ethyl]benzamide (39)—The title compound was obtained as described in the general procedure using DMF/CH₂Cl₂ (1:1) as a solvent in 73% yield (white solid). ¹H NMR (400 MHz, CD₃OD and CDCl₃): δ 8.55 (d, 1H, *J* = 2.4 Hz), 8.22 (d, 1H, *J* = 8.4 Hz), 8.21 (d, 1 H, 8.4 Hz), 7.90 (d, 1H, *J* = 7.9 Hz), 7.83 (d, 1H, *J* = 8.1 Hz), 7.64–7.46 (m, 5H), 7.43 (br d, *J* = 8.2 Hz), 6.16 (m, 1H), 4.38 and 4.32 (AB, 2H, *J* = 11.5 Hz), 2.92 (s, 3H), 1.81 (d, 3H, *J* = 6.8 Hz).

5-Amino-2-methoxymethyl-N-[1-methyl-1-(1-naphthyl)ethyl]benzamide (40)—The title compound was obtained as described for compound **24** in 82% yield (slightly yellow solid). ¹H NMR (400 MHz, CDCl₃): δ 8.24 (d, 1H, *J* = 8.3 Hz), 7.97 (br d, 1H, *J* = 7.7 Hz), 7.88 (d, 1H, *J* = 8.0 Hz), 7.80 (d, 1H, *J* = 8.1 Hz), 7.60–7.43 (m, 4H), 7.15 (d, 1H, *J* = 2.5 Hz), 7.00 (d, 1H, *J* = 8.1 Hz), 6.65 (dd, 1H, *J* = 8.1, 2.5 Hz), 6.15 (m, 1H), 4.08 and 4.02 (AB, 2H, *J* = 10.2 Hz), 3.80 (br s, 2H), 2.70 (s, 3H), 1.77 (d, 3H, *J* = 6.8 Hz); ¹³C NMR (100 MHz, CDCl₃): δ 167.1, 146.9, 138.5, 138.0, 133.9, 132.8, 131.2, 128.7, 128.2, 126.5, 125.8, 125.2, 123.6, 123.2, 122.6, 116.2, 73.2, 56.8, 44.8, 20.4. MS (EI): *m/z* 334.20 [M]⁺; HRMS (EI), calcd for C₂₁H₂₂N₂O₂ 334.1681, found [M]⁺ 334.1679.

5-Amino-2-methylbenzoic acid methyl ester (41)—To a solution of nitro **35** (635 mg, 3.3 mmol) in EtOAc (10 mL) was added 10% Pd-C (30 mg) and it was allowed to stir for 16 h at 23 °C under H₂ atmosphere. The reaction was filtered through celite pad and the filtrate was concentrated under reduced pressure. The residue was purified by silica gel column chromatography to furnish compound **41** (536 mg, >99%) as a colorless oil, *R_f* = 0.57 (hexane: EtOAc = 1:1), ¹H NMR (400 MHz, CDCl₃): δ 7.21 (d, 1H, *J* = 2.5 Hz), 6.97 (d, 1H, *J* = 8.1 Hz), 6.69 (dd, 1H, *J* = 2.5 and 8.1 Hz), 3.82 (s, 3H), 3.64 (s, 2H), 2.43 (s, 3H); ¹³C NMR (100 MHz, CDCl₃): δ 168.1, 144.1, 132.3, 129.8, 129.5, 118.8, 116.7, 51.6, 20.6. MS (EI): *m/z* 165.20 [M]⁺; HRMS (EI), calcd for C₉H₁₁NO₂ 165.0790, found [M]⁺ 165.0787.

2-Methyl-5-cyanobenzoic acid methyl ester (42)—CuCN (228 mg, 2.5 mmol) was suspended in distilled water (2 mL). NaCN (353 mg, 7.2 mmol) was added with vigorous stirring and the internal temperature was kept below 40 °C until all the CuCN went into solution. A suspension of amine **41** (350 mg, 2.1 mmol), in water (4 mL) and conc. HCl (0.7 mL) was stirred and cooled in an ice bath. When the temperature reach 5 °C, a solution of NaNO₂ (190 mg, 2.8 mmol) in water (0.6 mL) was added dropwise at 5 °C. When all the NaNO₂ was added, the solution was added dropwise the NaCN/CuCN solution at 0 °C. A few drops of methanol were added to keep the foaming under control. Stirring was continued for 3 h at 23 °C. The suspension was extracted with EtOAc and the organic layers were dried over Na₂SO₄ and concentrated under reduced pressure. The residue was purified by silica gel column chromatography to give compound **42** (115 mg, 31%) as a colorless oil, *R_f* = 0.63 (hexane: EtOAc = 1:1), ¹H NMR (400 MHz, CDCl₃): δ 8.08 (d, 1H, *J* = 1.7 Hz), 7.56 (dd, 1H, *J* = 1.7 and 7.9 Hz), 7.28 (d, 1H, *J* = 7.9 Hz), 3.83 (s, 3H), 2.56 (s, 3H); ¹³C NMR (100 MHz, CDCl₃): δ 165.7, 145.5, 134.4, 134.1, 132.4, 130.3, 117.8, 109.7, 52.1, 21.8.

5-*N*-*TERT*-Butoxycarbonylmethylamino-2-methylbenzoic acid methyl ester (43)—To a solution of nitrile **42** (40 mg, 0.23 mmol) in MeOH (1.5 mL) was added Boc₂O (0.1 mL, 0.46 mmol) and NiCl₂·6H₂O (5.4 mg, 0.022 mmol) at 0 °C. NaBH₄ (61 mg, 1.6 mmol) was then added in small portions over 15 min. The reaction was allowed to stir for 2 h at 23 °C. At this point, diethylenetriamine (25 μL, 0.23 mmol) was added. The mixture was allowed to stir for 15 min. The solvent was removed and the residue was dissolved with EtOAc. The organic layer was washed with saturated NaHCO₃ solution and dried over Na₂SO₄. The solvent was removed under reduced pressure to give a residue which was purified by silica gel column chromatography to furnish compound **43** (54 mg, 85%) as a colorless oil, *R*_f = 0.49 (hexane: EtOAc = 3:1), ¹H NMR (400 MHz, CDCl₃): δ 7.78 (s, 1H), 7.29 (d, 1H, *J* = 7.8 Hz), 7.17 (d, 1H, *J* = 7.8 Hz), 4.92 (bs, 1H), 4.26 (d, 2H, *J* = 5.7 Hz), 3.85 (s, 3H), 2.53 (s, 3H), 1.42 (s, 9H); ¹³C NMR (100 MHz, CDCl₃): δ 167.8, 155.8, 139.2, 136.5, 132.0, 131.3, 129.4, 129.5, 79.5, 51.8, 44.0, 28.3, 21.3. MS (CI): *m/z* 278.30 [M]⁺; HRMS (CI), calcd for C₁₅H₂₀NO₄ 278.1392, found [M - H]⁺ 278.1398.

5-(*N,N*-*TERT*-Butoxycarbonylmethyl)methylamino-2-methylbenzoic acid methyl ester (44)—To a solution of *N*-Boc amine **43** (60 mg, 0.21 mmol) in THF (3 mL) was added dropwise 0.5M KHMDS in toluene (0.64 mL, 0.32 mmol) at 0 °C under argon atmosphere and it was allowed to stir for 30 min at 0 °C. The mixture was added dropwise MeI (21 μL, 0.34 mmol) at 0 °C and it was allowed to stir for 16 h at 23 °C. The reaction was quenched with saturated NH₄Cl solution and extracted with EtOAc. The organic layers were dried over Na₂SO₄ and concentrated under reduced pressure. The residue was purified by silica gel column chromatography to give compound **44** (52 mg, 83%) as a colorless oil, *R*_f = 0.60 (hexane: EtOAc = 3:1), ¹H NMR (400 MHz, CDCl₃): δ 7.75 (s, 1H), 7.24 (bs, 1H), 7.17 (d, 1H, *J* = 7.8 Hz), 4.36 (bs, 2H), 3.85 (s, 3H), 2.80 and 2.74 (each s, 3H), 2.54 (s, 3H), 1.45 (s, 9H); ¹³C NMR (100 MHz, CDCl₃): δ 167.8, 155.6, 139.1, 135.6, 131.9, 131.2, 130.8, 129.5, 79.8, 51.7, 33.8, 28.3, 21.3.

5-*N*-*TERT*-Butoxycarbonylmethylamino-2-methylbenzoic acid (45)—To a solution of ester **43** (54 mg, 0.19 mmol) in a mixture (9:1) of THF and water (2 mL) was added LiOH·H₂O (12 mg, 0.29 mmol) at 0 °C and it was allowed to stir for 16 h at 23 °C. The reaction was concentrated under reduced pressure and the residue was diluted with saturated NaHCO₃ solution. The mixture was extracted with Et₂O and the aqueous layer was acidified with 1M HCl solution to pH 4. The white solid was extracted with EtOAc and the organic layers were dried over Na₂SO₄, and concentrated under reduced pressure to provide corresponding acid **45** (39 mg, 76%) as a white solid, *R*_f = 0.51 (CH₂Cl₂: MeOH = 9:1), ¹H NMR (300 MHz, CDCl₃): δ 7.78 (s, 1H), 7.27 (d, 1H, *J* = 7.8 Hz), 7.15 (d, 1H, *J* = 7.8 Hz), 4.78 (bs, 1H), 4.19 (s, 2H), 2.50 (s, 3H), 1.40 (s, 9H); ¹³C NMR (75 MHz, CDCl₃): δ 170.8, 158.0, 139.5, 135.3, 132.5, 131.4, 130.2, 129.7, 80.1, 44.2, 28.7, 21.6.

5-*N*-*TERT*-Butoxycarbonylmethylamino-2-methyl-*N'*-[(*R*)-1-(1-naphthyl)ethyl]benzamide (47)—The title compound was obtained as described in the general procedure in 91% yield (white solid). *R*_f = 0.20 (hexane: EtOAc = 3:1), ¹H NMR (300 MHz, CDCl₃): δ 8.20 (d, 1H, *J* = 8.4 Hz), 7.85 (d, 1H, *J* = 7.5 Hz), 7.78 (d, 1H, *J* = 8.4 Hz), 7.58-7.40 (m, 4H), 7.13 (d, 2H, *J* = 7.5 Hz), 7.08 (d, 1H, *J* = 7.8 Hz), 6.15-6.06 (bm, 2H), 4.86 (bs, 1H), 4.14 (d, 2H, *J* = 5.1 Hz), 2.36 (s, 3H), 1.75 (d, 3H, *J* = 6.0 Hz), 1.39 (s, 9H); ¹³C NMR (75 MHz, CDCl₃): δ 168.7, 155.8, 137.9, 136.5, 136.5, 134.9, 133.9, 131.1, 128.7, 128.7, 128.4, 127.2, 126.5, 125.9, 125.5, 125.1, 123.5, 122.5, 79.5, 44.8, 43.9, 28.3, 20.6, 19.3. MS (EI): *m/z* 418.45 [M]⁺; HRMS (EI), calcd for C₂₆H₃₀N₂O₃ 418.2256, found [M]⁺ 418.2252.

5-(*N,N*-*TERT*-Butoxycarbonylmethyl)methylamino-2-methyl-*N'*-[(*R*)-1-(1-naphthyl)ethyl]benzamide (48)—The title compound was obtained as described for compound **45** and general procedure in 98% yield as 2 steps (white solid). $R_f = 0.20$ (hexane: EtOAc = 3:1), $[\alpha]_D^{20} -46.3$ ($c=1$, CHCl_3); $^1\text{H NMR}$ (300 MHz, CDCl_3): δ 8.22 (d, 1H, $J = 8.1$ Hz), 7.85 (d, 1H, $J = 7.5$ Hz), 7.78 (d, 1H, $J = 8.4$ Hz), 7.58-7.40 (m, 4H), 7.11 (d, 1H, $J = 7.2$ Hz), 6.16-6.05 (m, 1H), 6.04 (bs, 1H), 4.28 (s, 2H), 2.71 (s, 3H), 2.38 (s, 3H), 1.76 (d, 3H, $J = 6.3$ Hz), 1.39 (s, 9H); $^{13}\text{C NMR}$ (75 MHz, CDCl_3): δ 168.8, 155.5, 137.8, 136.6, 135.6, 134.9, 133.0, 131.1, 128.8, 128.7, 128.4, 127.2, 126.5, 125.9, 125.6, 125.1, 123.5, 122.5, 79.6, 51.9, 44.7, 33.8, 28.3, 20.5, 19.4. MS (ESI): m/z 455.99 $[\text{M} + \text{Na}]^+$; HRMS (ESI), calcd for $\text{C}_{27}\text{H}_{32}\text{N}_2\text{O}_3\text{Na}$ 455.2311, found $[\text{M} + \text{Na}]^+$ 455.2312.

***N*-methyl-5-methylamino-2-methyl-*N'*-[(*R*)-1-(1-naphthyl)ethyl]benzamide (49)**—The title compound was obtained as described for compound **9** in 76% yield (white solid). $R_f = 0.27$ (CH_2Cl_2 : MeOH = 9:1), $[\alpha]_D^{20} -71.5$ ($c=1$, MeOH); $^1\text{H NMR}$ (300 MHz, CDCl_3 plus a small amount of CD_3OD): δ 8.25 (d, 1H, $J = 8.1$ Hz), 7.88 (d, 1H, $J = 8.4$ Hz), 7.79 (d, 1H, $J = 8.4$ Hz), 7.63 (d, 1H, $J = 7.3$ Hz), 7.59-7.44 (m, 3H), 7.25 (d, 2H, $J = 7.8$ Hz), 7.17 (d, 1H, $J = 7.8$ Hz), 6.05 (q, 1H, $J = 6.9$ Hz), 3.61 (s, 2H), 2.32 (s, 3H), 2.31 (s, 3H), 1.69 (d, 3H, $J = 6.9$ Hz); $^{13}\text{C NMR}$ (75 MHz, CDCl_3 plus a small amount of CD_3OD): δ 171.9, 140.3, 138.1, 137.8, 135.7, 135.5, 132.4, 131.8, 130.9, 129.9, 129.0, 128.2, 127.3, 126.7, 126.5, 124.3, 123.8, 55.7, 46.3, 35.5, 21.4, 19.4. MS (EI): m/z 332.30 $[\text{M}]^+$; HRMS (EI), calcd for $\text{C}_{22}\text{H}_{24}\text{N}_2\text{O}$ 332.1889, found $[\text{M}]^+$ 332.1891.

5-methylamino-2-methyl-*N'*-[(*R*)-1-(1-naphthyl)ethyl]benzamide (2)—The title compound was obtained as described for compound **9** in 56% yield (white solid). $R_f = 0.11$ (CH_2Cl_2 : MeOH = 9:1), $^1\text{H NMR}$ (400 MHz, CDCl_3 plus a small amount of CD_3OD): δ 8.14 (d, 1H, $J = 8.5$ Hz), 7.78 (d, 1H, $J = 8.0$ Hz), 7.69 (d, 1H, $J = 8.2$ Hz), 7.52 (d, 1H, $J = 7.1$ Hz), 7.47-7.34 (m, 3H), 7.16-7.15 (m, 2H), 7.06 (d, 1H, $J = 8.2$ Hz), 5.93 (q, 1H, $J = 6.8$ Hz), 3.61 (s, 2H), 2.21 (s, 3H), 1.59 (d, 3H, $J = 6.8$ Hz); $^{13}\text{C NMR}$ (100 MHz, CDCl_3 plus a small amount of CD_3OD): δ 172.0, 140.9, 140.3, 138.1, 135.5, 135.3, 132.4, 131.9, 129.9, 130.0, 129.0, 127.3, 127.1, 126.7, 126.5, 124.3, 123.7, 46.3, 46.0, 21.4, 19.3. MS (EI): m/z 318.30 $[\text{M}]^+$; HRMS (EI), calcd for $\text{C}_{21}\text{H}_{22}\text{N}_2\text{O}$ 318.1732, found $[\text{M}]^+$ 318.1734.

Computational Material and Methods

Docking—A genetic algorithm implemented in GOLD v3.2²⁵, was used to dock 46 inhibitors into the active site of the ligand bound form of the SARS-CoV PLpro crystal structure (PDB id: 3e9s)¹³. All ligand and water molecules except five, namely HOH2555, HOH2563 (conserved), HOH2590 (conserved), HOH2574, and HOH2595 (conserved) were deleted from the crystal structure of the ligand-bound form of the protease. Polar hydrogen atoms were added using the Sybyl package.²⁶ The 46 ligands were drawn using Chem 3D-Ultra 9.0. These structures were minimized in Sybyl7.3 by molecular mechanics with the Tripos force field to a gradient of 0.005 kcal/(mol Å), after addition of hydrogen atoms to the ligands. The crystal structure co-ordinates of the bound ligand, **24**, were used as a reference molecule for docking the other 45 compounds in GOLDDv3.2 which allows full ligand flexibility and automatic consideration of cavity bound water molecules. The genetic algorithm parameters were all set to default except the number of the operations were increased to 500000 and the population size was incremented to 500. If the top three conformations generated by the docking software for the ligands did not differ from each other by at least 1.5Å, early termination was allowed, ensuring non-redundant ligand conformations. The five water molecules were explicitly defined in the docking configuration file and were integral to the docking procedure and results. The top three conformations were saved for further analysis. The best scoring ligand conformation was

determined as the final docked conformation for each of the 46 ligands and was used for the alignment in the proceeding QSAR analysis.

CoMSIA—The final top scoring docked conformations of the 46 molecules were retrieved from the GOLDv3.2 run. Mulliken charges were calculated for these fully optimized structures based on the AM1 method in the Sybyl distribution of MOPAC. The resulting charged 46 molecules were aligned to each other for the CoMSIA analyses to explore the specific contributions of the effect of physicochemical properties on their bioactivities. By virtue of their similar docked conformations in the active site of SARS-PLpro, the overall alignment did not need much manual tuning. Using the QSAR module in Sybyl, a spreadsheet was created for the 46 aligned molecules. Five physicochemical properties namely, steric, electrostatic, hydrophobic fields, and hydrogen bond donor and acceptor were evaluated. Similarity indices were computed using a probe with a charge of +1, radius of 1 Å, a hydrophobicity of +1. The default value of 30 kcal/mol was set as the maximum cut-off for steric and electrostatic energies. With standard options for variable scaling, SAMPLE method, leave-one-out cross validations were performed to determine the optimal principal component number. The cross-validation runs were carried out for 20 groups and the 10 round bootstrap run followed. The final CoMSIA model was obtained with this optimal number of components and non-cross validated conventional correlations. The training set was further tuned to delete five outlier compounds; this improved the model's q^2 value considerably. Hence, the resulting CoMSIA model training set consisted of 41 molecules including compound **24**.

SARS-CoV PLpro Purification and IC₅₀ Value Determination—The SARS-CoV PLpro enzyme (residues 1541–1855) was expressed and purified from *E. coli* according to our previously reported procedures.^{11d} IC₅₀ values for all inhibitors were determined using a 96-wellplate-based assay similar to our previously described methods.¹¹ The substrate used in the assay was the fluorogenic peptide Arg-Leu-Arg-Gly-Gly-AMC (RLRGG-AMC) which was purchased from Bachem Bioscience. Reactions were performed in a total volume of 50 µL which contained the following components: 50 mM HEPES, pH 7.5, 0.1 mg/mL BSA, 5 mM DTT, 50 µM RLRGG-AMC, 2% DMSO, and varying concentrations of inhibitor (0–200 µM). Reactions were initiated with the addition of PLpro to produce a final enzyme concentration of 125 nM. Reaction progress was monitored continuously on a Tecan Genios Pro microplate reader ($\lambda_{\text{excitation}}=360$ nm; $\lambda_{\text{emission}}=460$ nm; gain=40). Initial rate data were fit to the equation $v_i = v_o/(1 + [I]/IC_{50})$ using the Enzyme Kinetics module of SigmaPlot (v. 9.01 Systat Software, Inc.) where v_i is the reaction rate in the presence of inhibitor, v_o is the reaction rate in the absence of inhibitor, and $[I]$ is the inhibitor concentration.

Supplementary Material

Refer to Web version on PubMed Central for supplementary material.

Acknowledgments

This work was supported by the Public Health Service Research Grant P01 AI060915 (“Development of Novel Protease Inhibitors as SARS Therapeutics”).

Abbreviations

SARS	severe acute respiratory syndrome
SARS-CoV	SARS-coronavirus 3CLpro, chymotrypsin-like protease

PLpro	papain-like protease
WHO	world health organization
QSAR	quantitative structural activity relationship
CoMSIA	comparative molecular similarity indices analysis

References

1. World Health Organization. Communicable Disease Surveillance & Response, website. http://www.who.int/csr/sars/archive/2003_05_07a/en and http://www.who.int/csr/sars/country/en/coutry2003_08_15.pdf
2. Drosten C, Gunther S, Preiser W, van der Werf S, Brodt HR, Becker S, Rabenau H, Panning M, Kolesnikova L, Fouchier RA, Berger A, Burguiere AM, Cinatl J, Eickmann M, Escriou N, Grywna K, Kramme S, Manuguerra JC, Muller S, Rickerts V, Sturmer M, Vieth S, Klenk HD, Osterhaus AD, Schmitz H, Doerr HW. Identification of a novel coronavirus in patients with severe acute respiratory syndrome. *N Engl J Med.* 2003; 348:1967–1976. [PubMed: 12690091]
3. (a) Ksiazek TG, Erdman D, Goldsmith CS, Zaki SR, Peret T, Emery S, Tong S, Urbani C, Comer JA, Lim W, Rollin PE, Dowell SF, Ling AE, Humphrey CD, Shieh WJ, Guarner J, Paddock CD, Rota P, Fields B, DeRisi J, Yang JY, Cox N, Hughes JM, LeDuc JW, Bellini WJ, Anderson LJ. A novel coronavirus associated with severe acute respiratory syndrome. *N Engl J Med.* 2003; 348:1953–1966. [PubMed: 12690092] (b) Peiris JS, Lai ST, Poon LL, Guan Y, Yam LYC, Lim W, Nicholls J, Yee WKS, Yan WW, Cheung MT, Cheng VC, Chan KH, Tsang DN, Yung RWH, Ng TK, Yuen KY. Coronavirus as a possible cause of severe acute respiratory syndrome. *Lancet.* 2003; 361:1319–1325. [PubMed: 12711465]
4. Li W, Shi Z, Yu M, Ren W, Smith C, Epstein JH, Wang H, Crameri G, Hu Z, Zhang H, Zhang J, McEachern J, Field H, Daszak P, Eaton BT, Zhang S, Wang LF. Bats are natural reservoirs of SARS-like coronaviruses. *Science.* 2005; 310:676–679. [PubMed: 16195424]
5. Lau SKP, Woo PCY, Li KSM, Huang Y, Tsoi HW, Wong BHL, Wong SSY, Leung SY, Chan KH, Yuen KY. Severe acute respiratory syndrome coronavirus-like virus in Chinese horseshoe bats. *Proc Natl Acad Sci USA.* 2005; 102:14040–14045. [PubMed: 16169905]
6. He JF, Peng GW, Min J, Yu DW, Liang WJ, Zhang SY, Xu RH, Zheng HY, Wu XW, Xu J, Wang ZH, Fang L, Zhang X, Li H, Yan XG, Lu JH, Hu ZH, Huang JC, Wan ZY, Hou JL, Lin JY, Song HD, Wang SY, Zhou XJ, Zhang GW, Gu BW, Zheng HJ, Zhang XL, He M, Zheng K, Wang BF, Fu G, Wang XN, Chen SJ, Chen Z, Hao P, Tang H, Ren SX, Zhong Y, Guo ZM, Liu Q, Miao YG, Kong XY, He WZ, Li YX, Wu CI, Zhao GP, Chiu RWK, Chim SSC, Tong YK, Chan PKS, Tam JS, Lo YMD. Molecular evolution of the SARS-coronavirus during the course of the SARS epidemic in China. *Science.* 2004; 303:1666–1669. [PubMed: 14752165]
7. Baker, SC. *Encyclopedia of Virology.* 3. Vol. 1. 2008. Coronaviruses: Molecular Biology; p. 554-562.
8. Ghosh AK, Xi K, Johnson ME, Baker SC, Mesecar AD. Progress in Anti-SARS Coronavirus Chemistry, Biology and Chemotherapy. *Annual Reports in Med Chem.* 2006; 41:183–196. (b) Yang H, Bartlam M, Rao Z. Drug Design Targeting the Main Protease, the Achilles' Heel of Coronaviruses. *Curr Pharm Des.* 2006; 12:4573–4590. [PubMed: 17168763]
9. (a) Ghosh AK, Xi K, Grum-Tokars V, Xu X, Ratia K, Fu W, Houser KV, Baker SC, Johnson ME, Mesecar AD. Structure-based design, synthesis, and biological evaluation of peptidomimetic SARS-CoV 3CLpro inhibitors. *Bioorg Med Chem Lett.* 2007; 17:5876–5880. [PubMed: 17855091] (b) Jain RP, Pettersson HI, Zhang J, Aull KD, Fortin PD, Huitema C, Eltis LD, Parrish JC, James MNG, Wishart DS, Vederas JC. Synthesis and Evaluation of Keto-Glutamine Analogues as Potent Inhibitors of Severe Acute Respiratory Syndrome 3CLpro. *J Med Chem.* 2004; 47:6113–6434. [PubMed: 15566280] (c) Vederas JC, Jain RP. Structural variations in keto-glutamines for improved inhibition against hepatitis A virus 3C proteinase. *Bioorg Med Chem Lett.* 2004; 14:3655. [PubMed: 15203137]

10. (a) Devaraj SG, Wang N, Chen Z, Chen Z, Tseng M, Barretto N, Lin R, Peters CJ, Tseng CTK, Baker SC, Li K. Regulation of IRF-3-dependent Innate Immunity by the Papain-like Protease Domain of the Severe Acute Respiratory Syndrome Coronavirus. *J Biol Chem.* 2007; 282:32208–32221. [PubMed: 17761676] (b) Ratia K, Saikatendu KS, Santarsiero BD, Barretto N, Baker SC, Stevens RC, Mesecar AD. Severe acute respiratory syndrome coronavirus papain-like protease: Structure of a viral deubiquitinating enzyme. *Proc Natl Acad Sci USA.* 2006; 103:5717–5722. [PubMed: 16581910] (c) Barretto N, Jukneliene D, Ratia K, Chen Z, Mesecar AD, Baker SC. The Papain-Like Protease of Severe Acute Respiratory Syndrome Coronavirus Has Deubiquitinating Activity. *J Virol.* 2005; 79:15189–15198. [PubMed: 16306590]
11. (a) Lindner HA, Fotouhi-Ardakani N, Lytvyn V, Lachance P, Sulea T, Ménard R. The Papain-Like Protease from the Severe Acute Respiratory Syndrome Coronavirus Is a Deubiquitinating Enzyme. *J Virol.* 2005; 79:15199–15208. [PubMed: 16306591] (b) Sulea T, Lindner HA, Purisima EO, Ménard R. Deubiquitination, a New Function of the Severe Acute Respiratory Syndrome Coronavirus Papain-Like Protease? *J Virol.* 2005; 79:4550–4551. [PubMed: 15767458]
12. Ziebuhr J, Schelle B, Karl N, Minskaia E, Bayer S, Siddell SG, Gorbalenya AE, Thiel V. Human Coronavirus 229E Papain-Like Proteases Have Overlapping Specificities but Distinct Functions in Viral Replication. *J Virol.* 2007; 81:3922–3932. [PubMed: 17251282]
13. Ratia K, Pegan S, Takayama J, Sleeman K, Coughlin M, Chaudhuri R, Fu W, Prabhakar BS, Johnson ME, Baker SC, Ghosh AK, Mesecar AD. A noncovalent class of papain-like protease/deubiquitinase inhibitors blocks SARS virus replication. *Proc Natl Acad Sci USA.* 2008; 105:16119–16124. [PubMed: 18852458]
14. Mu F, Coffing SL, Riese DJ II, Geahlen RL, Verdier-Pinard P, Hamel E, Johnson J, Cushman M. Design, Synthesis, and Biological Evaluation of a Series of Lavendustin A Analogues That Inhibit EGFR and Syk Tyrosine Kinases, as Well as Tubulin Polymerization. *J Med Chem.* 2001; 44:441–452. [PubMed: 11462983]
15. Yokoyama N. *Eur Pat Appl.* 1988:EP284297.
16. Yang Q, Ney JE, Wolfe JP. Palladium-Catalyzed Tandem N-Arylation/Carboamination Reactions for the Stereoselective Synthesis of N-Aryl-2-benzyl Pyrrolidines. *Org Lett.* 2005; 7:2575–2578. [PubMed: 15957894]
17. Ciganek E. Tertiary carbinamines by addition of organocerium reagents to nitriles and ketimines. *J Org Chem.* 1992; 57:4521–4527.
18. Kraszkievicz L, Sosnowski M, Skulski L. Oxidative Iodination of Deactivated Arenes in Concentrated Sulfuric Acid with I₂/NaIO₄ and KI/NaIO₄ Iodinating Systems. *Synthesis.* 2006:1195–1199.
19. Wang L, Wang GT, Wang X, Tong Y, Sullivan G, Park D, Leonard NM, Li Q, Cohen J, Gu WZ, Zhang H, Bauch JL, Jakob CG, Hutchins CW, Stoll VS, Marsh K, Rosenberg SH, Sham HL, Lin NH. Design, Synthesis, and Biological Activity of 4-[(4-Cyano-2-arylbenzyloxy)-(3-methyl-3H-imidazol-4-yl)methyl]benzonnitriles as Potent and Selective Farnesyltransferase Inhibitors. *J Med Chem.* 2004; 47:612–626. [PubMed: 14736242]
20. Sderberg BC, Chisnell AC, O'Nei SN, Shriver JA. Synthesis of Indoles Isolated from *Tricholoma* Species. *J Org Chem.* 1999; 64:9731–9734.
21. Biasotti B, Dallavalle S, Merlini L, Farina C, Gagliardi S, Parini C, Belfiore P. Synthesis of photoactivable inhibitors of osteoclast vacuolar ATPase. *Bioorg Med Chem.* 2003; 11:2247–2254. [PubMed: 12713834]
22. Caddick S, Judd DB, Lewis AK, de K, Reich MT, Williams MRV. A generic approach for the catalytic reduction of nitriles. *Tetrahedron.* 2003; 59:5417–5423.
23. See supporting information
24. Klebe G, Abraham U, Mietzner T. Molecular Similarity Indices in a Comparative Analysis (CoMSIA) of Drug Molecules To Correlate and Predict Their Biological Activity. *J Med Chem.* 1994; 37:4130–4146. [PubMed: 7990113]
25. Jones G, Willett P, Glen RC, Leach AR, Taylor R. Development and validation of a genetic algorithm for flexible docking. *J Mol Biol.* 1997; 267:727–748. [PubMed: 9126849]
26. SYBYL v.7.3 Tripos International, 1699 South Hanley Rd., St. Louis, Missouri, 63144, USA.

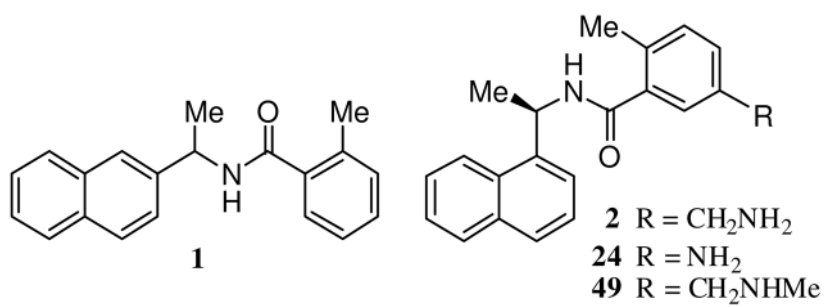


Figure 1.
Structure of inhibitors 1, 2, 24 and 4

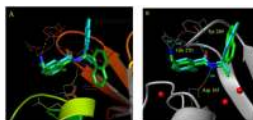


Figure 2.

Docking in the presence of conserved water molecules is critical for replicating the binding conformation of inhibitors in the active site of the bound form of SARS-CoV PLpro. (A) Docking of compound **2** in the **absence of water molecules** in the active site of the inhibitor-bound form of SARS-CoV PLpro causes the naphthyl rings to flip down into a pocket, as shown by the docked conformation of compound **2** (in green) when compared to the crystal structure conformation of compound **24** (in cyan). In the x-ray structure of compound **24**, the naphthyl rings are flipped up in the opposite direction, holding the flexible loop in place. The yellow dotted lines show the possible interactions of the docked compound **2** with residues Tyr269, Gln270 and Asp165 (catalytic domain residue numbering). (B) The three conserved water molecules are marked; two of them are buried deep in the pocket (P5) whereas the third one lies in a groove between residues Lys158 and Glu168. The position of these water molecules is integral to structure-based inhibitor design efforts. The crystal structure conformation of compound **24** is shown in cyan whereas the docked conformation of compound **2** in the presence of water molecules (red dots) is shown in green.

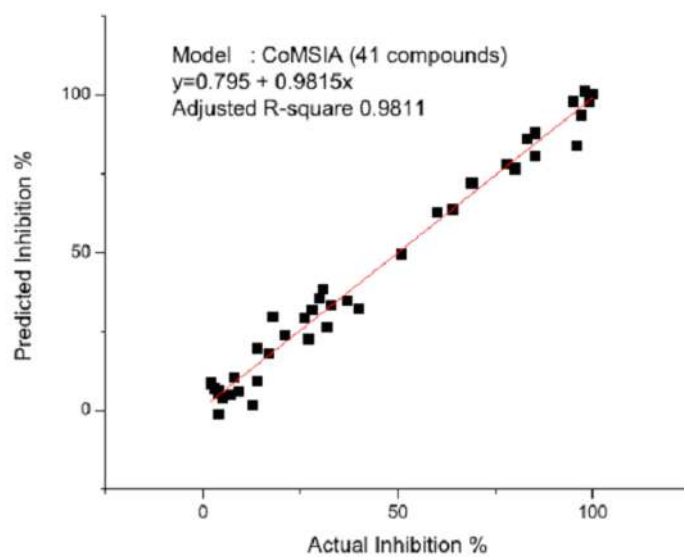


Figure 3. Correlation plot between the predicted percent inhibition of 41 compounds and the actual experimental percent inhibition values obtained at 100 μ M.

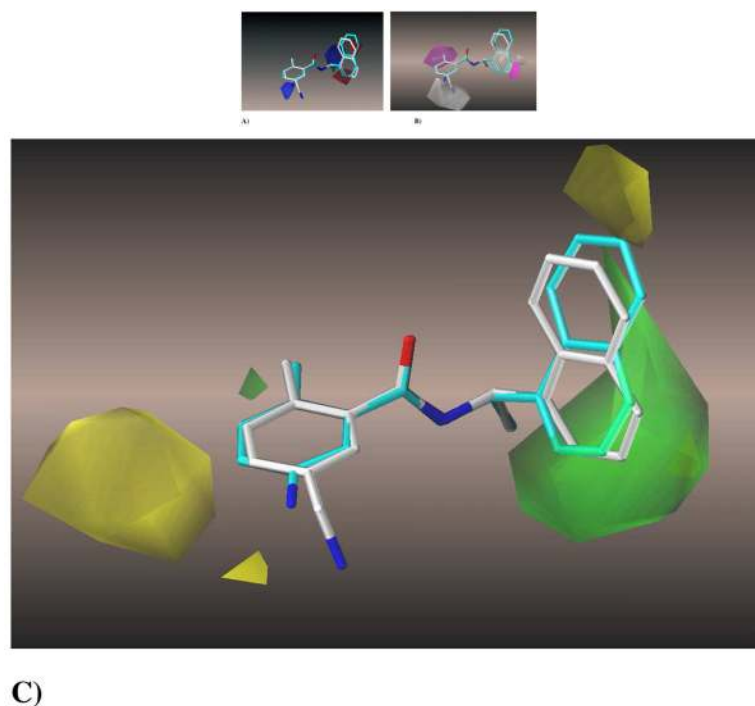
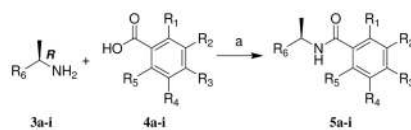


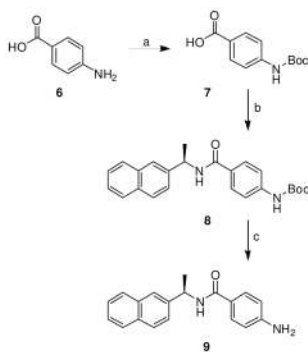
Figure 4. Compound **24** is shown in cyan in its bound conformation as in the crystal structure aligned with the docked conformation of the most active compound **2**, in white, when docked in the presence of 3 conserved water molecules. A) The electrostatic contour map for this series of SARS-CoV PLpro inhibitors. Blue is the region of unfavorable negative charge and red is of favorable negative charge. B) The hydrophobic contour map, where white is the region of unfavorable lipophilic interactions and magenta is of favorable lipophilicity. C) A steric contour map, with green denoting the region of favorable steric interactions and yellow denoting unfavorable regions.

**Scheme 1.**

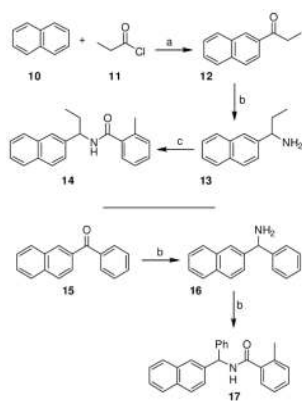
Reagents and conditions: (a) EDCI, HOBT, DIPEA, 23 °C, 16 h.

compounds	R ₁	R ₂	R ₃	R ₄	R ₅	R ₆
5a	H	Me	H	H	H	2-naphthyl
5b	H	H	Me	H	H	2-naphthyl
5c	OMe	H	H	H	H	2-naphthyl
5d	H	OMe	H	H	H	2-naphthyl
5e	H	H	OMe	H	H	2-naphthyl
5f	Me	H	H	H	Me	2-naphthyl ^a
5g	OH	H	H	H	H	2-naphthyl
5h	Me	H	H	H	H	1-naphthyl
5i	Me	H	H	NO ₂	H	1-naphthyl

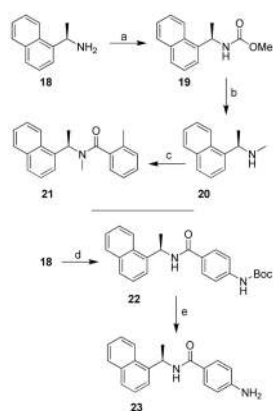
^aDMF was used as solvent; CH₂Cl₂ was used in all other reactions.

**Scheme 2.**

Reagents and conditions: (a) Boc_2O , Et_3N , dioxane/ H_2O (2:1), 23 °C, 16 h; (b) (*R*)-(+)-1-(2-naphthyl)ethan-1-amine, EDCI, HOBT, DIPEA, CH_2Cl_2 , 23 °C, 16 h; (c) TFA, CH_2Cl_2 , 23 °C, 2 h.

**Scheme 3.**

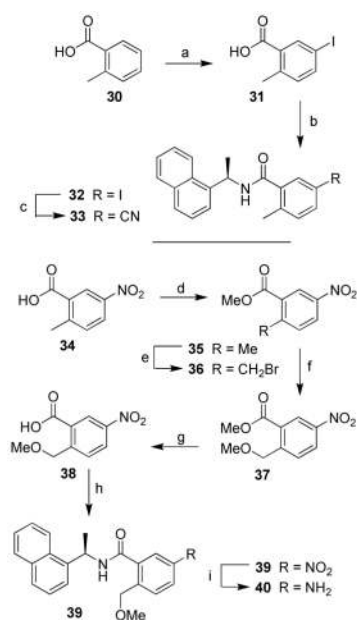
Reagent and conditions: (a) AlCl_3 , 1,2-dichloroethane, 35 °C, 4 h; (b) NH_4OAc , NaBH_3CN , MeOH, 23 °C, 24 h; (c) *o*-toluic acid, EDCI, HOBT, DIPEA, DMF, 23 °C, 16 h; (d) *o*-toluic acid, EDCI, HOBT, DIPEA, CH_2Cl_2 , 23 °C, 16 h.

**Scheme 4.**

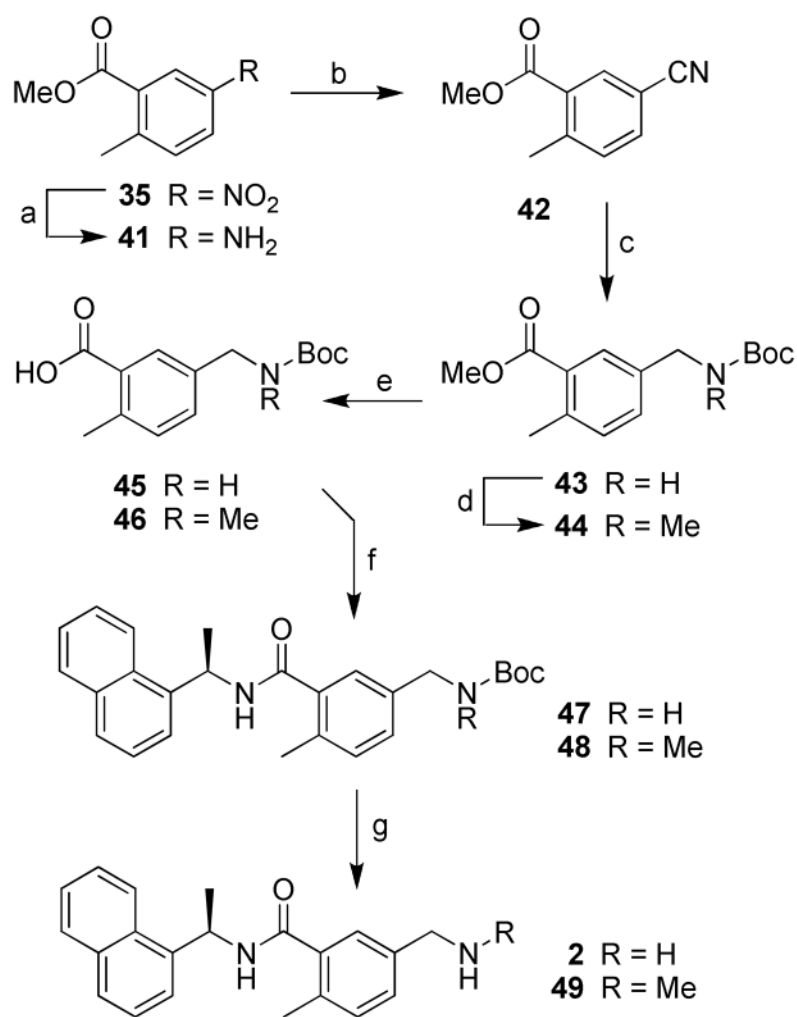
Reagents and conditions: (a) ClCO_2Me , K_2CO_3 , dioxane/ H_2O (1:1), 0 °C, 1 h; (b) LiAlH_4 , THF, reflux, 1 h; (c) *o*-toluic acid, EDCI, HOBT, DIPEA, DMF, 23 °C, 16 h; (d) 7, EDCI, HOBT, DIPEA, DMF, 23 °C, 16 h; (e) TFA, CH_2Cl_2 , 23 °C, 2 h.

**Scheme 5.**

Reagents and conditions: (a) H₂, Pd-C, EtOAc/MeOH (1:1), 23 °C, 15 h; (b) Ac₂O, Et₃N, CH₂Cl₂, 23 °C, 18 h; (c) MeLi, CeCl₃, THF, 23 °C, 2 h; (d) 2-Methyl-5-nitrobenzoic acid, EDCI, HOBT, DIPEA, CH₂Cl₂, 23 °C, 16 h; (e) H₂, Pd-C, EtOAc/MeOH (1:1), 23 °C, 15 h.

**Scheme 6.**

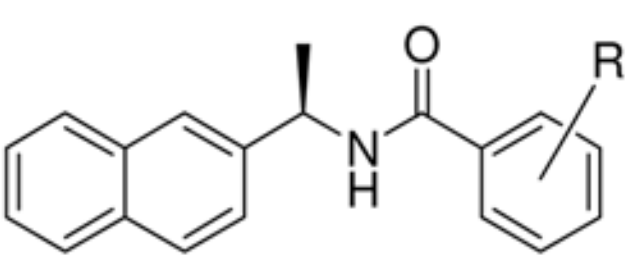
Reagents and conditions: (a) KI, NaIO₄, conc. H₂SO₄, 25–30 °C, 2 h; (b) (*R*)-(+)-1-(1-naphthyl)ethylamine **18**, EDCI, HOBT, DIPEA, DMF/CH₂Cl₂ (1:1), 23 °C, 48 h; (c) CuCN, KCN, DMF, 130 °C, 16 h; (d) SOCl₂, MeOH, reflux, 4 h; (e) NBS, Bz₂O₂, CCl₄, reflux, 24 h; (f) NaH, NaOMe, MeOH, 50 °C, 4 h; (g) LiOH·H₂O, THF/H₂O (5:1), 23 °C, 1.5 h; (h) (*R*)-(+)-1-(1-naphthyl)ethylamine **18**, EDCI, HOBT, DIPEA, DMF/CH₂Cl₂ (1:1), 23 °C, 16 h; (i) H₂, Pd-C, EtOAc, 23 °C, 10 h.

**Scheme 7.**

Reagents and conditions: (a) H₂, Pd-C, EtOAc, 23 °C, 16 h; (b) NaNO₂, conc. HCl, CuCN, NaCN, H₂O, 23 °C, 3 h; (c) Boc₂O, NiCl₂·6H₂O, NaBH₄, MeOH, 23 °C, 2 h; (d) MeI, KHMDS, THF, 23 °C, 16 h; (e) LiOH·H₂O, THF/H₂O (9:1), 23 °C, 16 h; (f) (*R*)-(+)-1-(1-naphthyl)ethylamine **18**, EDCI, HOBT, DIPEA, CH₂Cl₂, 23 °C, 16 h; (g) TFA, CH₂Cl₂, 23 °C, 2 h.

Table 1

Structure and activity of substituted benzamide derivatives

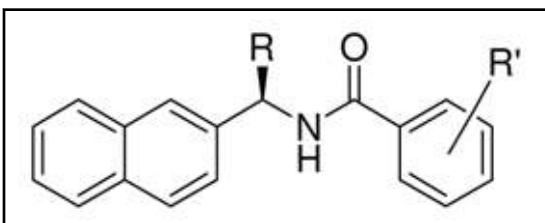


compound	R	IC ₅₀ (μM)
lead	2-Me	8.7 ± 0.7
5a	3-Me	14.8 ± 5.0
5b	4-Me	29.1 ± 3.8
5c	2-OMe	90 ± 26
5d	3-OMe	13.5 ± 6.8
5e	4-OMe	149 ± 43

(IC₅₀ = enzyme inhibitory activity)

Table 2

Structure and activity of naphthyl and benzamide derivatives

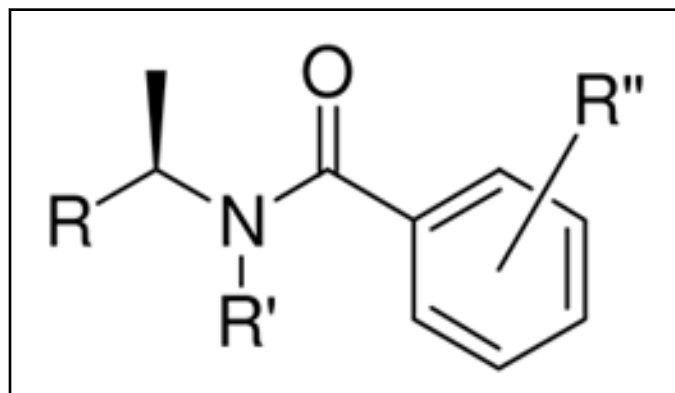


compound	R	R'	IC ₅₀ (μM)
lead	Me	2-Me	8.7 ± 0.7
5f	Me	2,6-diMe	12.1 ± 0.7
5g	Me	2-OH	N/A
9	Me	4-NH ₂	46.1 ± 13.0
8	Me	4-Boc-NH	N/A
14	Et (racemic)	2-Me	N/A
17	Ph (racemic)	2-Me	N/A

(IC₅₀ = enzyme inhibitory activity)

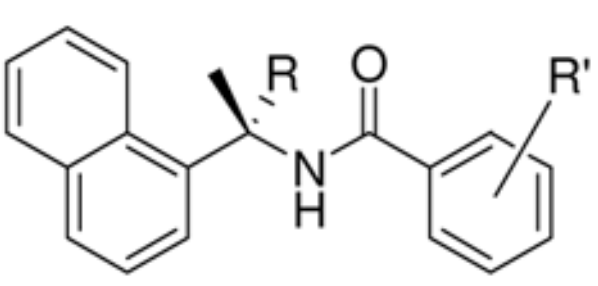
Table 3

Structure and activity of 1-, 2-naphthalene and benzamides



compound	R	R'	R''	IC ₅₀ (μM)
Lead	2-Naphthyl	H	2-Me	8.7 ± 0.7
5h	1-Naphthyl	H	2-Me	2.3 ± 0.1
21	1-Naphthyl	Me	2-Me	22.6 ± 6.9
23	1-Naphthyl	H	4-NH ₂	24.8 ± 1.0
24	1-Naphthyl	H	2-Me and 5-AcNH	0.56 ± 0.03
25	1-Naphthyl	H	2-Me and 5-NH ₂	2.64 ± 0.04

(IC₅₀ = enzyme inhibitory activity)

Table 4Structure and activity of substituted benzamide derivatives And an α -disubstituted naphthyl derivative


compound	R	R'	IC ₅₀ (μM)
24	H	2-Me and 5-NH ₂	0.56 ± 0.03
29	Me	2-Me and 5-NH ₂	11.1 ± 1.3
33	H	2-Me and 5-CN	5.2 ± 0.5
40	H	2-CH ₂ OMe and 5-NH ₂	2.7 ± 0.1
32	H	2-Me and 5-I	1.4 ± 0.3
47	H	2-Me and 5-CH ₂ NHBoc	4.8 ± 0.4
49	H	2-Me and 5-CH ₂ NHMe	1.3 ± 0.1
2	H	2-Me and 5-CH ₂ NH ₂	0.46 ± 0.03

(IC₅₀) = enzyme inhibitory activity)

Table 5

Evaluation of compounds as inhibitors of SARS-CoV replication in a cell-based assay.

Compound	IC ₅₀ (μM)	EC ₅₀ (μM)
1	20.1 ± 1.1	NI*
2	0.46 ± 0.03	6.0 ± 0.1
lead	8.7 ± 0.7	NI
5a	14.8 ± 5.0	NI
24	0.56 ± 0.03	14.5 ± 0.8
25	2.64 ± 0.04	13.1 ± 0.7
29	11.1 ± 1.3	NI
47	4.8 ± 0.4	NI
49	1.3 ± 0.1	5.2 ± 0.3

(IC₅₀ = enzyme inhibitory activity; EC₅₀ = antiviral activity; NI = no inhibition)